AD-A127 357 EXAMINATION OF THE FEASIBILITY OF DETECTION OF CALCIUM 1/
EVAPORATION FROM A..(U) AIR FORCE INST OF TECH
WRIGHT-PATTERSON AFB OH SCHOOL OF ENGI.. V L EASON
UNCLASSIFIED MAR 83 AFIT/GNE/PH/83M-6 F/G 7/4 NL

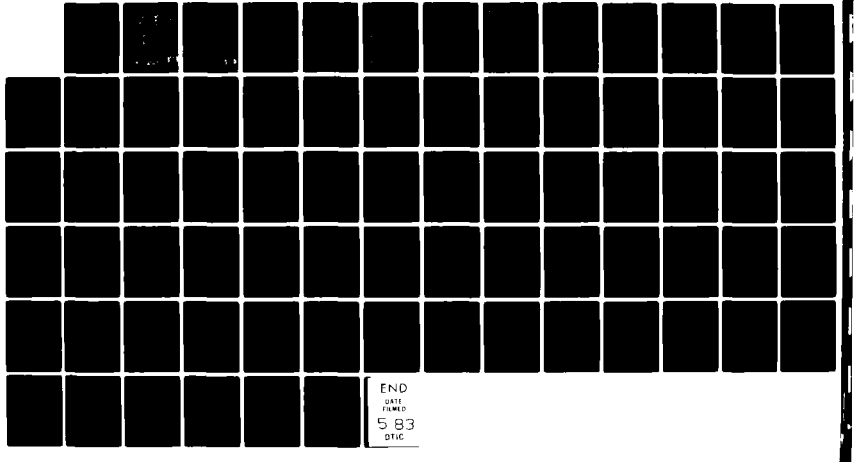

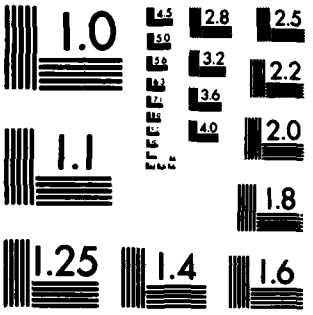

AIR FORCE INSTITUTE OF TECHNOLOGY

AIR UNIVERSITY
UNITED STATES AIR FORCE

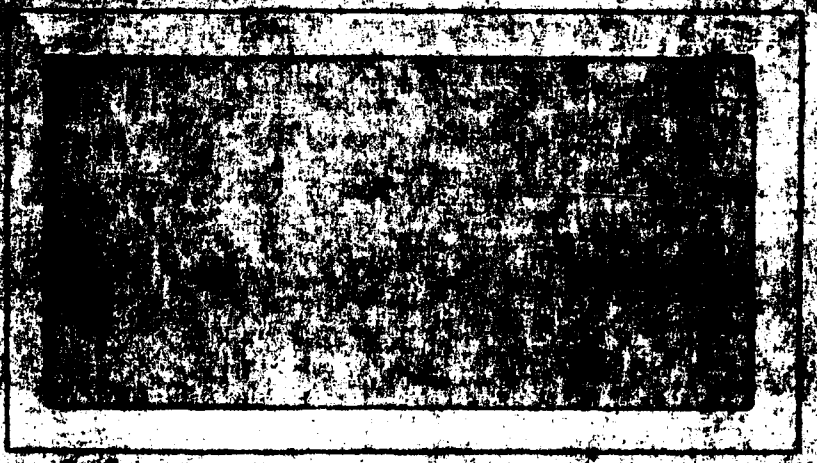

SCHOOL OF ENGINEERING

WRIGHT-PATTERSON AIR FORCE BASE, OHIO

EXAMINATION OF THE FEASIBILITY OF DETECTION OF CALCIUM EVAPORATION FROM A TYPE B DISPENSER CATHODE BY LASER INDUCED PHENOMENA

THESIS

AFIT/GNE/PH/83M-6

Virginia L. Eason
Lieutenant USN

Approved for public release: distribution unlimited

AFIT/GNE/PH/83M-6

EXAMINATION OF THE FEASIBILITY OF DETECTION OF CALCIUM EVAPORATION FROM A TYPE B DISPENSER CATHODE BY LASER INDUCED PHENOMENA

THESIS

Presented to the Faculty of the School of Engineering
of the Air Force Institute of Technology
Air University
in Partial Fulfillment of the
Requirements for the Degree of
Master of Science

by
Virginia L. Eason, B.S. Physics
Lieutenant USN
Graduate Nuclear Engineering
March 1983

Approved for public release: distribution unlimited

Acknowledgments

I would like to thank my advisor, Dr. T. E. Luke, for his guidance and support throughout my thesis effort. Dr. W. B. Roh was especially helpful and patient in explaining aspects of laser physics that were unfamiliar to me. Dr. R. L. Hengehold answered many questions and aided me in locating equipment on numerous occasions. Two laboratory assistants, Mr. Ron Gabriel and Mr. Don Elworth, provided useful technical information and saved me many hours by providing excellent logistical support. Finally, I would like to thank Capt. E. F. Kasper who most graciously kept me briefed on the daily progress of his experiments and allowed me access to his laboratory so that I was able to begin my experiment smoothly.

Virginia L. Eason

Contents

List of Figures

List of Tables

Abstract

Three methods, laser induced resonance fluorescence, excitation to a shorter lived level from a metastable level, and ionization spectroscopy are examined for feasibility of detecting and measuring calcium evaporation from a type B cathode. Laser induced fluorescence of the $4s^1S_0 \leftrightarrow 4p^1P_1$ (4226 Å) transition of calcium is the most promising and the easiest to implement. Ionization of the calcium atoms after they have been excited by a laser to the metastable $^3P_1$ state is feasible but requires redesign of extant equipment to implement. Excitation to a shorter lived level from the metastable $^3P_1$ state is feasible for the transition from the $^3D_2$ (4435 Å) level and not feasible for the $^3S_1$ (6122 Å) transition. Sensitized fluorescence and stimulated emission involving excited calcium atoms is examined and discarded. Calcium evaporation rates are semi-quantitatively related to barium evaporation rates to take advantage of the more extensive literature on the latter. Limited experimental data is presented which indicates that an observation reported by another researcher of the barium evaporation rate decreasing after the cathode exceeded 1200° K is not attributable to pulse pile up error in the photon counting system but is most likely attributable to a cathode physics phenomenon. An argument for switching the course of future experiments from evaporation rates vs lifetime studies to evaporation rate vs cathode temperature is made. All calculations are based upon

experimental results of previous workers and are order of magnitude rather than a rigorous treatment.

EXAMINATION OF THE FEASIBILITY OF DETECTION OF CALCIUM EVAPORATION FROM A TYPE B DISPENSER CATHODE BY LASER INDUCED PHENOMENA

I. Introduction

The military communications satellite program projects a need for traveling wave tubes (TWTs) with a current generation and lifetime capacity exceeding present tubes (Ref 1:5). Present cathode technology cannot meet the projected requirements. J. L. Cronin of Spectra Mat (Ref 2:23) has flatly stated that the cathode industry probably cannot produce such a cathode within a few years either. His assessment is probably accurate since past cathode improvements have relied on empirical data and serendipity. No definitive theory of cathode physics exists which reliably predicts cathode behavior as a function of construction and manufacturing processes. Reliance on past methods of cathode improvement will not suffice to meet the stringent performance criteria expected of space-born TWTs. It is not even known if the projected requirements are physically feasible. A viable theory of cathode physics is sorely needed.

Background on Cathodes and Their Operation

Rather than relate the entire history of cathode development here, the interested reader may find an excellent rendition by Cronin (Ref 2). Only the essentials which bear directly upon the problem this thesis addresses are mentioned.

A cathode generates current by thermionic emission. The cathode is indirectly heated (Figure 1) and electrons are emitted

from the cathode. The Richardson-Dushman equation in its simplest form relates the current density to the temperature as:

$$J = AT^2 e^{-\phi/kT} \quad (1)$$

where

J is the current density (A/cm^2)

A is the thermionic Richardson constant

T is the temperature (°K)

ϕ is the work function (eV)

k is Boltzman's constant

From Eq (1) it is obvious that by decreasing the work function or increasing the temperature, the current density can be increased. The temperature at which the cathode operates cannot be indefinitely increased to obtain any desired current density because too high a temperature has a deleterious effect on cathode life. Practical tradeoffs must be made between cathode temperature and current density. Lowering the work function is the most desirable way to increase the current density and cathode life.

Modern cathodes are either the dispenser type B (Figure 1) or a variation of it. The B type consists of a porous tungsten plug mounted in a refractory sleeve, usually molybdenum, through which the additives in the reservoir can diffuse to the surface of the cathode. The additives serve to lower the work function at the surface. The object of the variations to the type B cathode is to lower the work function still further and/or extend the life of the additives. Extant variations fall into three basic

categories:

(1) Variation of the molar proportions of additives

(2) Variation of porosity of tungsten matrix

(3) Coating of cathode with thin films of refractory metals (osmium-ruthenium or osmium-iridium)

Additionally, experimental work is being carried out in a fourth category:

(4) Mixing the tungsten matrix with osmium, rhenium, or iridium.

The additives used to lower the work function are the Group II aluminates. Some combinations in common use are (Ref 3:1):

Composition (Mole Ratio)		
BaO	CaO	Al_2O_3
4	1	1
5	3	2
5	0	2
2	1	1
3	1	1
1	1	1

Historically the $5BaO$, $3CaO$, $2Al_2O_3$, henceforth referred to as either the 5:3:2 or type B cathode, is meant when the type B cathode is referred to. It is the 5:3:2 cathode which is treated in this thesis. Subsequent mention of "the cathode" refers to this type unless stated otherwise.

It is the barium, calcium, and oxygen which appear to be

the active elements in lowering the cathode work function and prolonging its life. The additives are introduced into the reservoir as barium and calcium aluminates because BaO and CaO alone are hygroscopic. The chemical reaction which produces free calcium and barium is presented later.

Although there is some disagreement (Ref 4,5,6), the preponderance of research tends to support the following statements about dispenser cathode characteristics:

(1) A barium monolayer completely covers the cathode except for the pores in the tungsten (Ref 7,8,9,10:383, 11:255).

(2) There is a monolayer of oxygen between the barium monolayer and the tungsten surface (Ref ibid).

(3) There is a partial understanding of how the monolayer decreases the work function in terms of chemisorption of an electropositive species and a resultant dipole layer (Ref 1:67-75).

(4) Barium evaporates from the surface or pores of the cathode and is replaced by barium from within the reservoir (Ref 12:398).

(5) The barium monolayer coverage of the cathode is maintained throughout cathode life (Ref 9:434C, 13:173).

(6) The initial evaporation rate of additives from a new cathode is large and falls off steeply in the first hundred or so hours of operation. Then barium and calcium depletion rates relax as $t^{-1/2}$ and $t^{-1/3}$ respectively (Ref 14, 15:2898).

(7) Calcium serves to slow the barium evaporation rate (Ref 2:19, 15:2898).

(8) Surface studies show that after the initial burst of evaporants (probably a result of the detritus left on the surface by manufacturing process), the surface contains only barium, oxygen, and tungsten (Ref 16:287). Calcium is conspicuously absent from the surface above 1500° K. Jones reported that calcium was absent in evaporants of the type B and M cathodes (Ref 11:255) while Sickafus failed to find calcium in pore deposits (Ref 17:218-219).

(9) The cathode fails when the additive reservoir is depleted (Ref 9:4345).

(10) There is no agreement of the transport mechanism by which barium arrives at the surface. Rittner suggests Knudsen flow (Ref 8:1471) while Brodie suggests migration (Ref 14:161).

There are three probable reasons why there is disagreement among the different researchers. The first is the difficulty of replicating a working vacuum tube environment. Depending upon the characteristics each researcher is exploring, the tube environment may be more or less faithfully reproduced. For instance, surface studies preclude placing the anode at the normal distance from the cathode whereas current versus time studies can be conducted without disturbing the tube environment. Partial pressures of residual gases are known to have a significant effect on tube lifetime; experimental conditions do not replicate the

environment of manufactured tubes. The second reason for disagreement is that different researchers have used different techniques to study cathodes. Different experimental approaches have led to conflicting results probably as a result of the environment replication problems just mentioned. Third is the tacit assumption that characteristics such as barium/calcium evaporation rates, replenishment rates, current density, and cathode life differ only by degree and not mechanism between oxide coated cathodes; B,L,M dispenser cathodes; and impregnated cathodes. Perhaps the falsity of this assumption explains why calcium has been consistently observed in the evaporants from all calcium aluminate impregnated cathodes but not in the evaporants from all the modern B dispenser cathodes. Furthermore, there is some ambiguity about the difference between dispenser and impregnated cathodes. Earlier "the reservoir" was mentioned. The reservoir can mean either a void beneath the tungsten plug or it may mean the interstices of the tungsten plug. When the interstices constitute the reservoir, cathodes are referred to as impregnated dispenser types (See Figure 1). Pressed cathodes, where the tungsten and additives were mixed together and pressed to form a plug, look like but do not function like impregnated cathodes. The haziness of cathode nomenclature should make a researcher wary of correlating results. For example, Sickafus (Ref 17:213) refers to "dispenser cathodes" which presumablyare impregnated and exhibit a barium evaporation rate which is proportional to $t^{-1/2}$. Rutledge calls a cathode, which is not impregnated, a

"dispenser cathode" and concludes that barium evaporation is proportional to 1/t (Ref 18:836).

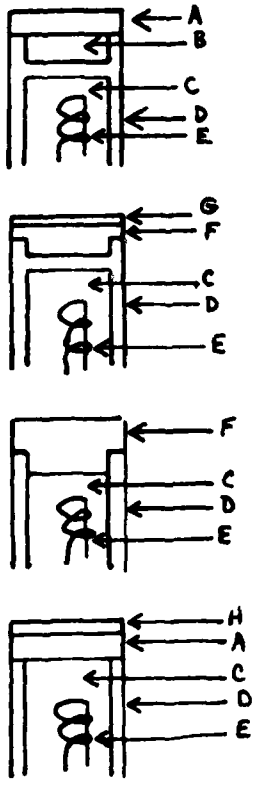

L type dispenser (Ref 19)

M type dispenser (Ref 2)

Modern B,S,A type dispenser (Ref 3)

Oxide coated

A: Porous tungsten plug

B: Reservoir for additives

C: Al_2O_3 potting

D: Molybdenum sleeve

E: Heater Filament

F: Impregnated porous tungsten plug

G: Osmium-ruthenium, osmium-iridium thin film

H: Group II oxide coating

Figure 1. Types of Cathodes

It is believed that the barium-oxygen monolayers on the surface are the primary agents in reducing the work function. Calcium is thought to play a role in retarding the barium evaporation rate but not in directly altering the work function (Ref 11:255). A model which explains the oxygen-barium monolayers bonding on the tungsten surface was presented by Green (Ref 20:42-68). Briefly, his model classifies metals into three categories based upon the geometric disposition of bonding orbitals at the metal surface. Category I metals (Mo, W) have vacant d-orbitals perpendicular to the surface. The bond which oxygen forms with the substrate metal distorts the oxygen valence electron configuration. As a result of the distortion, the barium-oxygen bond at the surface is covalent rather than the typical ionic bonding observed in bulk BaO crystals. A dipole moment is induced in the BaO layer with the positive side toward the external surface. Category II metals (Re, Os, Ir) enhance emission but do not form a dipole layer. Category III (Pt) degrades emission.

The model accounts for several experimental observations. Auger and x-ray photoelectron spectroscopy (XPS) data have shown that the chemical bond between Ba and O on the surface is not the same as that in bulk BaO and is in fact more covalent than ionic. The work function on different crystal planes on the surface are known to vary in what is commonly called patch effects. Patch effects could be construed to occur because of the extreme directionality of the covalent bonds and the resultant dipole moment. The model also successfully predicts which metals will

have good emissive characteristics and which will have poisoning effects. Combining Green's model with Jenkins' (Ref 21:354) discussion of activation by an electropositive contaminant produces insight into why the oxygen-barium monolayers are so successful in lowering the work function (Figures 2 and 3). Since

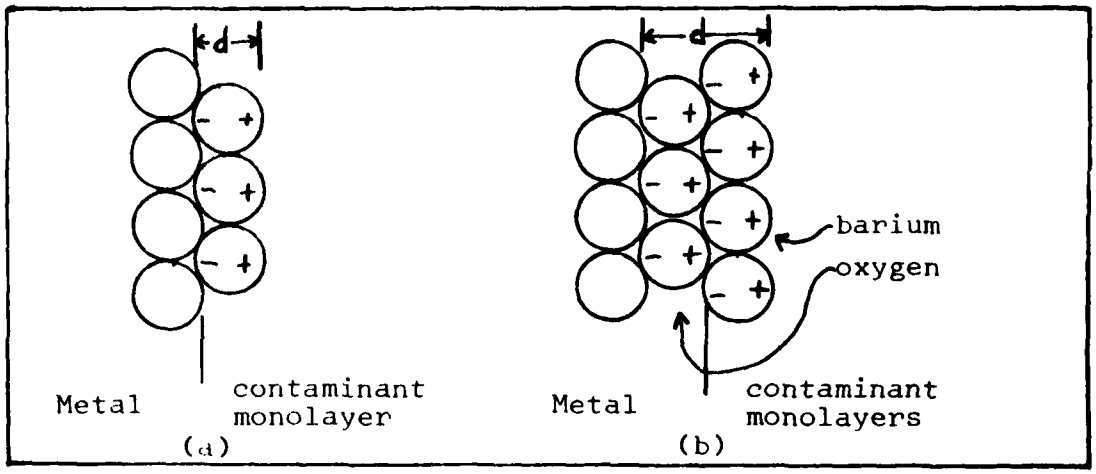

Figure 2. Dipole Monolayers (Ref 21: 354)

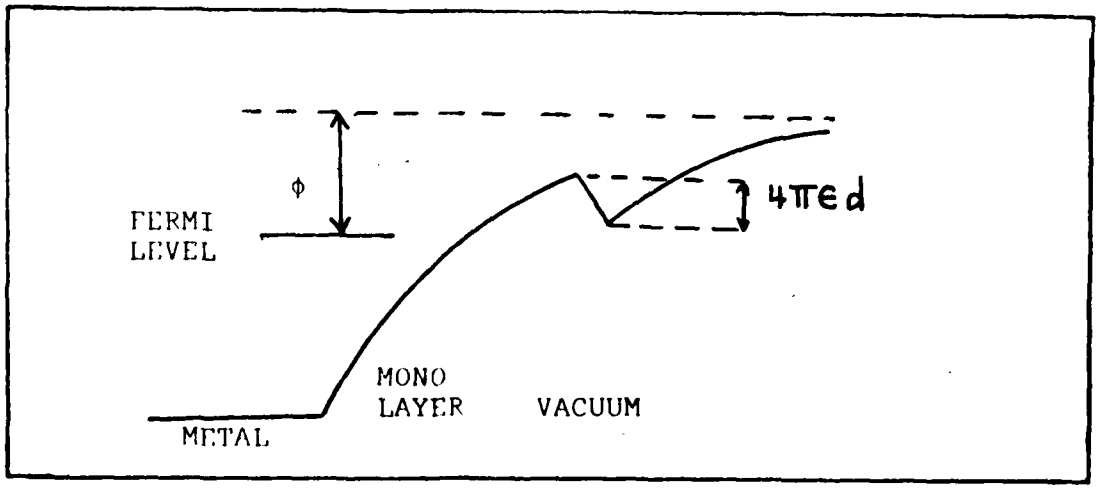

Figure 3. Potential Energy Diagrams for Metal Surfaces (Ref 21:354)

the reduction in work function is proportional to the dipole separation, d, (Ref 21:354) then the oxygen-barium monolayers are particularly effective, because d is larger for the oxygen-barium layer than for a single species monolayer. While Green's model provides a partial understanding of how barium reduces the work function, there is no analogous understanding of the barium and calcium replenishment/depletion mechanism. Barium evaporation has been more extensively studied than calcium. Evaporation studies to date have largely relied upon the Becker method. In the Becker approach, a clean tungsten wire is exposed to an evaporant stream which coats the wire. The wire is resistively heated to a low enough temperature to preclude evaporation of the coating. The thermionic emission from the wire is measured as a function of time. The maximum emission rate of the wire is proportional to the reciprocal of the barium evaporation rate from the cathode. The Becker method is combined with chemical analysis to produce absolute evaporation rates. There is some contention over the evaporation of calcium. Certain researchers have noted calcium depletion within the cathode, yet others have failed to find calcium on the cathode surface or in the evaporant stream of type B and M cathodes. Since it is the calcium and barium depletion which ultimately causes cathode failure, an understanding of the depletion mechanism could lead to improved cathodes.

Problem Statement and Scope

This thesis addresses the design of an experimental method to detect and quantitatively measure the instantaneous evaporation

rate of calcium from a dispenser cathode over the lifetime of the cathode. Three methods and their advantages and disadvantages are discussed. The methods were chosen on the basis of employing an extant experimental apparatus with a minimum of modifications. There is no attempt to treat the evaporant gas by quantum mechanical methods. Rather, order of magnitude calculations based on available data in the literature are made to illustrate the feasibility of each approach.

Assumptions

Since the body of experimental evidence for cathode behavior is in conflict, the assumptions employed throughout this paper are consolidated and presented here for convenience to the reader:

(1) Calcium evaporates from the calcium impregnated dispenser cathodes.

(2) The calcium evaporation rate is proportional to the depletion rate which follows a $t^{-1/3}$ decay.

(3) Calcium is not present on the cathode surface after the first few hours of life. It is present deep within the surface pores. Consequently, most of the escaping calcium gas leaves the cathode nearly perpendicularly.

(4) The calcium evaporation rate can be related to the barium evaporation rate.

(5) Quenching of laser excited atoms is minimal because

of the low pressure.

(6) The calcium evaporation rate that is calculated is taken to be smaller by 0.001 as a conservative estimate.

Order of Presentation

A discussion of the problem of detecting calcium is presented first. Direct laser induced fluorescence to measure the evaporation rate is examined (Ref 22, 23). Then a method of pumping the atoms in the metastable state to a shorter lived state is considered. Henceforth, this method is referred to as "double pumping". Next, the application of ionization spectroscopy methods are proposed. Other methods which were considered but discarded are briefly discussed. Methods to calibrate the laser wavelength, other than the optogalvanic effect, are briefly discussed. Recommendations for the direction of future experiments are given. Finally, conclusions and recommendations are stated.

II. Problem Analysis

Discussion of the Problem

Laser induced resonance fluorescence provides a method of obtaining absolute measurements of evaporant concentrations as low as 10^2-10^3 atoms/cm^3 (Ref 24:204, 25:27). Two previous workers (Ref 22, 23) successfully employed laser induced fluorescence to measure absolute barium evaporation rates from dispenser cathodes operating at various temperatures; both recommended application of the same techniques to measure calcium evaporation. Examination of Figure 4 reveals some constraints to the application of laser induced fluorescence to calcium which do not occur for barium. Of the two resonance transitions for calcium, the $4s^1S_0 \leftrightarrow 4p^1P_1$ (4226 Å) is difficult to work with because of dye laser instability and low output power in the 4200 Å region. The $4s^1S_0 \leftrightarrow 4p^3P_1$ (6573 Å) transition is easy to excite because the dye laser is stable and has sufficient output power to reach near saturation in the 6500 Å wavelength region, but $4p^3P_1$ state is most unfortunately metastable.

An initial attempt to detect calcium evaporating from a cathode by inducing laser fluorescence from the $^3P_1$ state was frustrated by two factors. First, the hollow cathode tube wavelength tuning method could not be used because the Ca hollow cathode tube is not responsive to the 6573 Å wavelength. Second, the $4p^3P_1$ state is metastable with a 0.39 m sec lifetime (Ref 28:75). Assuming that the calcium atoms leave the cathode perpendicularly (more will be said about this later), one degree

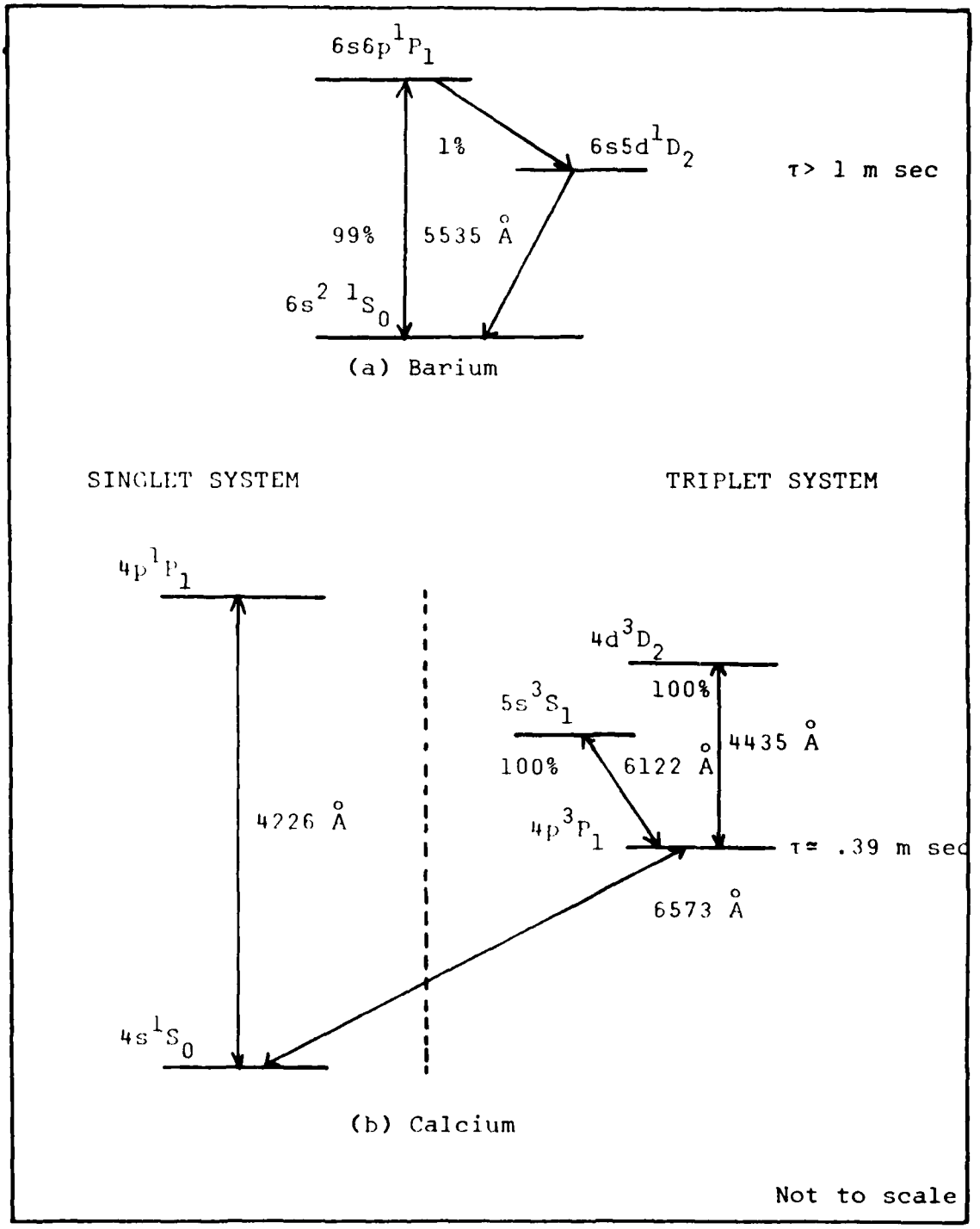

Figure 4. Partial Grotrian Diagrams for Calcium and Barium (Ref 26:340-358,27:E-341)

of freedom can be associated with the atomic kinetic energy. Thus, by the equipartition theorem, the velocity is given by the following equation:

$$Vrms = \sqrt{\frac{\frac{1}{2}kT}{m}} \qquad (2)$$

where

Vrms is the root mean square velocity (m/sec)

k is Boltzmann's constant

T is the temperature (°K)

m is the mass (kg)

If the cathode operates at 1050 °C, Vrms of Ca is about 524 m/sec. During the lifetime of the $4p^3P_1$ state, the average Ca atom will travel about 0.2 m before fluorescing. Since the test cell walls and cold finger are approximately 0.07 and 0.03 meters away from the cathode surface, the average Ca atom will de-excite by collision with the test cell or cold finger before it can fluoresce. Despite many attempts to observe fluorescence from the $4p^3P_1$ state by looking at a volume in the test cell just below the cold finger and using photomultiplier tubes of differing sensitivity to separate a weak signal from the noise, no fluorescence was detected.

The early frustrations in attempting to detect calcium are not deterrent enough to totally abandon laser induced fluorescence. There is strong motivation to seek some way to employ the apparatus used by Zemyan and Kasper because it is very sensitive, it was most successful in detection of barium, and the apparatus is available. The problem, then, is to seek modifications

to the apparatus or the detection technique which will allow the detection of calcium.

Criterion for Determining Feasibility of Proposed Experimental Approaches

The criterion for determining the feasibility of the proposed experimental methods depends upon the measurement of either fluorescent signal or ionization current. Specific values for the minimum detectable fluorescent signal or ionization current are derivable from expected calcium evaporation rate and experimental conditions.

The extant apparatus processes the data as illustrated in Figure 5a. The signal (SIG) is separated from the background (BKG) by synchronizing two counters in the photon counter/processor with a mechanical chopper which interrupts the laser beam (Figure 8). The signal is composed of the fluorescent counts and counts from the scattering of the laser in the test cell. Clearly, for the fluorescent signal to be measurable, the total signal must exceed the standard deviation of the background. Furthermore, the fluorescent signal must be distinguishable from the laser scatter signal. Blackbody radiation from the heated cathode is the overwhelming contributor to the background. The average blackbody contribution will depend on the cathode temperature and the wavelength at which the detection optics are tuned. Laser scatter can be minimized by altering the position of the cathode to the laser beam.

The question of the magnitude of the blackbody radiation at the wavelength of barium fluorescence (5535 Å) as opposed to

calcium fluorescence (4226 Å or 6122 Å) arises at this point. The Planck distribution is plotted in Figure 5b. The η values corresponding to wavelengths of interest are in the range of $17.79 < \eta < 28.39$ which is in the tail region of the curve. The η values were calculated from $\eta = h\omega/kT$ for 5535 Å at 1200° K (927° C) and for 6122 Å and 4226 Å at 1323° K (1050° C). It is worthwhile to compare the expected background at the rated type B cathode operating temperature (1323° K) to that noted by Kasper at 1200° K. Figure 5c is a plot of the Planck distribution in the range of interest. The background for 6122 Å and 4226 Å deviates from that of 5535 Å by $\pm$ 1 or 2 orders of magnitude. Since the standard deviation of the background for 5535 Å at 1200° K was found experimentally to be about 5×10^2 counts/sec when the cathode/beam separation is optimized to yield minimum scatter and maximum fluorescent count rate, an estimate of the detectable fluorescent count rate can be stated. At 6122 Å, the fluorescent count rate must exceed either 5×10^3 counts/sec (1200° K) or 5×10^4 counts/sec (1323°K). Similarly, at 4226 Å, the fluorescent count rate must exceed either 5×10^1 counts/sec (1200° K) or 5×10^2 counts/sec (1323° K).

The criterion of feasibility which is applied to the ionization approach is that the current produced is equal to or greater than 1 pico-Coulomb. The choice of 1 pico-Coulomb arises from the limitation of available current measuring devices.

Now that the general problem has been discussed and the criterion of feasibility set for each proposed approach, we can

Photon Counter		Components
DATA	=	SIG + BKG
BKG	=	Black Body + Light Leaks + Dark Counts
SUM	=	DATA + BKG
DIFF	=	DATA - BKG = Fluorescent Counts + Laser Scatter
SIG	=	Fluorescent Counts + Laser Scatter + Light Leaks + Dark Count + Black Body

(a) Photon Counter/Processor

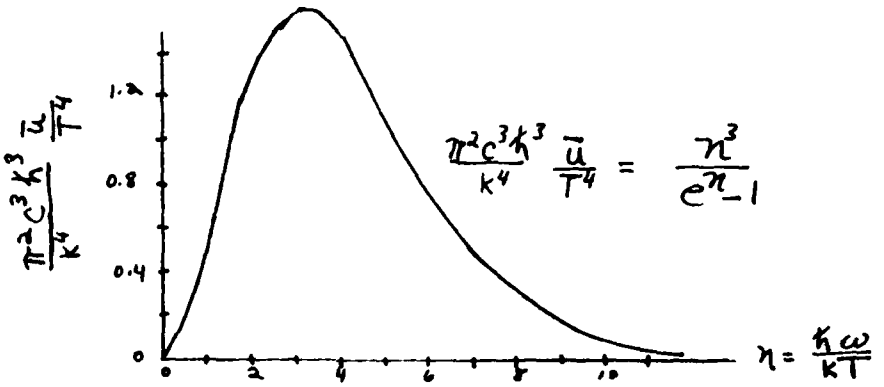

(b) Planck Energy Density

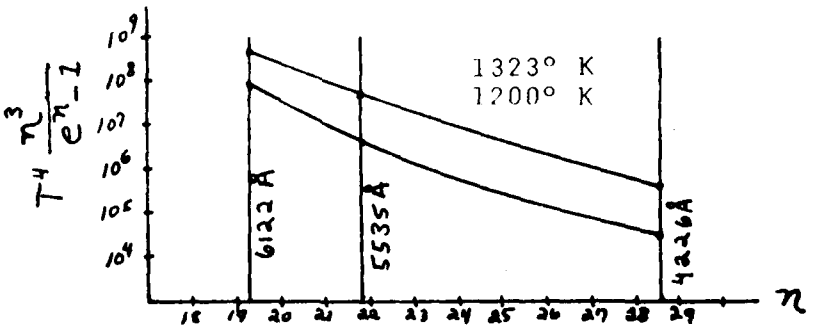

(c) Plot of Planck Curve for Visible Wavelength

Figure 5. Summary of Photon Counting Process

move on to a detailed description of each approach. The first approach is developed in the greatest detail with the analysis methods being carried over into the second approach. The general outline followed for each approach is as follows:

(1) Define the proposed experimental scheme

(2) Calculate the expected value of the measurable quantity

(3) Conclude the feasibility of the approach

(4) Delineate the changes in apparatus required and comment upon any difficulties

(5) Provide schematic of the apparatus

(6) Briefly describe the operation of the apparatus

Approach I. Induced Fluorescence of the $4s^1S_0 \longleftrightarrow 4p^1P_1$ (4226 Å) Transition

For the extant experimental apparatus (Figure 8), knowledge of three parameters is sufficient to determine the number of expected fluorescent counts: the number of atoms entering the beam, the detection capability of the optics, and available laser power. A reasonable estimate of the probable number of calcium atoms entering the laser beam can be made based upon the reported barium and calcium evaporation behavior. A typical value for the detection capability can be obtained from measurement of Rayleigh scattering off N_2 in the test cell. The available laser power is known from dye specifications and experience with R110 and R640 dyes used in the apparatus.

While there is a dearth of information in the literature on calcium evaporation rates, there is considerably more on barium evaporation rates. Based on the results of earlier work, it is possible to relate the calcium evaporation rate to the barium evaporation rate in a qualitative way. Palluel and Shroff reported that calcium and barium depletion rates from impregnated cathodes decrease as $t^{-1/3}$ and $t^{-1/2}$ respectively (Ref 15:2898). If it is assumed that the evaporation rate is proportional to the depletion rate, then

$$R_C = R_{Co} t^{-1/3} \tag{3}$$

and

$$R_B = R_{Bo} t^{-1/2} \tag{4}$$

where

R_C is evaporation rate of calcium (atoms/sec)

R_{Co} is an initial calcium evaporation rate (atoms/sec)

R_B is evaporation rate for barium (atoms/sec)

R_{Bo} is an initial barium evaporation rate (atoms/sec)

Taking the ratio of Eqs (3) and (4)

$$\frac{R_C}{R_B} = \frac{R_{Co}}{R_{Bo}} t^{1/6} \tag{5}$$

Equation (5) is not meant to be anything more than a qualitative estimate. Later it will be demonstrated that Eqs (3) and (4) are not too bad an assumption. The intent is to derive a reasonable estimate of the numbers of calcium atoms entering the laser beam throughout the cathode lifetime. Once the number entering the beam is known, the expected fluorescent count rate can be calculated and thence the feasibility of the measurement method throughout the cathode lifetime can be evaluated.

Since the evaporation rate does not relax to the depletion rate until after the first few hours of cathode operation, the time when it does was arbitrarily chosen as 100 hours (Ref 15: 2897. Also, the cathode being used had about 100 hours of operation time. From Brodie's data at 100 hours (Ref 14:158)

$$\frac{1}{(dq/dt)^2} = 150 \qquad \text{at } 1500^\circ \text{ K} \tag{6}$$

where

dq/dt is the evaporation rate of additives (monolayers/sec)

So converting to atoms/sec using the following equation

$$Ri = dq/dt \cdot MEAN \cdot A \cdot CF \tag{7}$$

where

Ri is evaporation rate of species (atoms/sec)

dq/dt is evaporation rate of additives (monolayers/sec)

MEAN is Brodie's mean for calcium and barium (4.8×10^{-9} and 7.3×10^{-8} g/cm^2- monolayer)

A is the cathode area (cm^2)

CF is a conversion factor $\left(\frac{6.02 \times 10^{23} \text{ atoms/mole}}{40.1 \text{ g/mole}}\right)$

We get roughly: $R_{Co} = 2.69 \times 10^{12}$ atoms/sec and $R_{Bo} = 4.09 \times 10^{13}$ atoms/sec.

Combining these values with Eq (5)

$$R_C \approx 0.07\ R_B t^{1/6} \qquad (8)$$

The basis for Eq (8) is Eqs (3) and (4). Just how reasonable was the assumption that the evaporation rates' dependence on time are represented by Eqs (3) and (4)? Ideally, if Eqs (3) and (4) are integrated over the cathode lifetime, the total quantity of evaporant should match the quantity of additive originally in the cathode. Practically, the match will not be exact. Factors which could make the integrated value less than the total are: the material that evaporated in the first 100 hours is not accounted for, and the additive reaction probably does not reach 100% completion. A factor which could make the integrated value larger than the total is the fact that Eqs (3) and (4) express evaporation rate as proportional to depletion rate. Depletion only means reduction of additive to a level below an average value in the "undepleted" region of the cathode reservoir. The constant of proportionality does not include an expression for the resistance to additive movement in the cathode. An arbitrary

cathode life of 40 K hour could yield an integrated value which is higher or lower than the total depending on how closely matched the arbitrary and actual lifetimes are.

The probable reaction which generates free barium and calcium gas from the cathode is (Ref 15:2899):

$$5\ BaO,\ 3\ CaO,\ 2\ Al_2O_3 + W \rightleftharpoons 2\ Ba\ Al_2\ O_4 \qquad (9)$$
$$+\ 3/4\ Ca_2\ Ba\ WO_6 + 1/4\ Ca_3\ WO_6 + 9/4\ Ba\ (g) + 3/4\ Ca(g)$$

Now if the average additive weight for a Semicon type B dispenser cathode is about 0.0325 gm (Ref 3), the right side of Eq (9) produces

$$\frac{120.3}{1137}(.0325\ gm) = 3.44 \times 10^{-3}\ gm\ Ca$$

and

$$\frac{686.5}{1137}(.0325\ gm) = 1.96 \times 10^{-2}\ gm\ Ba$$

Of the 5 moles of barium and 3 moles of calcium, only 9/4 and 3/4 respectively become gaseous, the rest being bound within the cathode. Thus, the total amount of gas expected is

$$\frac{.75}{3}(3.44 \times 10^{-3}\ gm) = 8.6 \times 10^{-4}\ gm\ of\ Ca\ (g)$$
$$or\ (1.29 \times 10^{19}\ Ca\ atoms)$$

and

$$\frac{2.25}{5}(1.96 \times 10^{-2}\ gm) = 8.82 \times 10^{-3}\ gm\ of\ Ba\ (g)$$
$$or\ (3.87 \times 10^{19}\ Ba\ atoms)$$

Integrating Eqs (3) and (4) and remembering to change R_{Bo} and R_{Co} to evaporation rates per hour

$$Ca\ (atoms) = \int_{100\ hr}^{40,000\ hr} R_{Co} t^{-1/3} dt \qquad (10)$$

$$\text{Ba (atoms)} = \int_{100\ \text{hr}}^{40{,}000\ \text{hr}} R_{Bo} t^{-1/2} dt \qquad (11)$$

which when evaluated yield 1.66×10^{19} Ca atoms and 5.6×10^{19} Ba atoms. These values are slightly larger than but of the same order of magnitude as those calculated to be the total number of Ba and Ca atoms liberated. In using the calculated values of R_{Bo} and R_{Co}, it should be noted too that Brodie's data was for 25% porous cathodes which exhibit greater evaporation rates than the modern 20% porous cathodes. Table I is a comparison of barium evaporation rates for different temperatures as measured by Zemyan and Kasper. They are about one thousandth of the calculated value of R_{Bo}. To be conservative, R_{Bo} and R_{Co} will be taken as one thousandth of their calculated values to account for the probable resistance to additive flow to the cathode surface, smaller porosity of modern cathodes, and the fact that the values were calculated for a cathode operating at 1500° K.

The foregoing discussion allows an estimate of 2.7×10^{9} Ca atoms evaporating from the cathode at t = 100 hours to be made. Eq (8) is still valid.

Not all the calcium atoms evaporating from the cathode enter the laser beam. To make an exact calculation of the average number of atoms entering the beam, the distribution function f (V, θ) of the evolving atoms must be known where V is the velocity and θ is the angle of departure from the cathode surface. An estimate rather than an exact calculation must suffice because f (V, θ) is not known. Assume that all the atoms entering the

Table I

Comparison of Barium Evaporation Rates

as a Function of Temperature

Approx Cathode Temp (°K)	R_{Ba} (Ref 22:50) (x 10^{10})(atoms/sec)	R_{Ba} (Ref 23:56) (x 10^{10})(atoms/sec)
900	2.0	3.7
950	2.7	3.8
1000	5.4	4.1
1050	7.8	4.4
1100	*	6.0
1200	*	6.7
1300	*	5.6

* Not reported

beam came from the area of the cathode directly beneath the beam. This is tantamount to saying that all the atoms evaporate perpendicularly from the cathode with no angular distribution. For calcium atoms, this is not a bad assumption of the results of recent studies, which state the absence if calcium from the cathode surface, are accepted as valid. Then, if there is no Ca on the surface, any calcium gas escaping the cathode must have evolved deep within the surface pores. If the pore axes are assumed to be parallel to the normal to the cathode surface, only those atoms moving parallel to the normal would escape. With the above assumption, the number of atoms entering the beam is

the above assumption, the number of atoms entering the beam is illustrated (Figure 6).

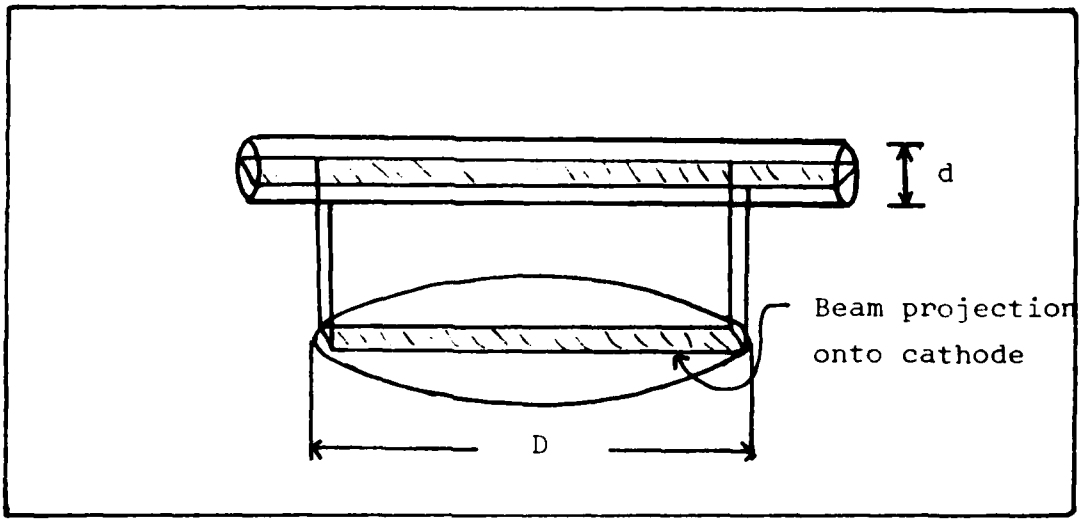

Figure 6. Cathode Beam Geometry

$$N = \text{TOTAL } N \cdot \frac{\text{PROJECTED AREA}}{\text{TOTAL AREA}} \qquad (12)$$

where

TOTAL N is 2.7×10^9 Ca atoms/sec

PROJECTED AREA is area of beam projection onto cathode

TOTAL AREA is total cathode area

Using the dimensions (D = 0.762 cm) of the cathode employed in the experiment (Ref 3) and a typical beam diameter of 0.5 mm (Ref 29), N is about 2.3×10^8 atoms/sec.

The detected fluorescent power for a particular transition is:

$$P_f = (\text{Number of detected fluorescent counts/sec}) \cdot (h\nu) \qquad (13)$$

and equating Eq (13) to Zemyan's Eq (13) (Ref 22:20)

$$D_f \cdot h\upsilon = S h\upsilon \; N_t v \; \frac{(V_c \Omega \varepsilon)}{8\pi^2 D} \tag{14}$$

where

D_f is number of detected fluorescent counts (counts/sec)

h is Planck's constant (joule-sec)

υ is the transition frequency (sec^{-1})

S is the average number of times an atom spontaneously radiates at the given frequency in passing through the beam

N_t is the number density of atoms ($atoms/cm^3$)

v is the root mean square atomic velocity (m/sec)

D is the beam diameter (m)

$V_c \Omega \varepsilon$ is related to the detection optics and detection efficiency

N_t is given in terms of the evaporation rate, velocity of escaping atoms, and cathode area as

$$N_t = \frac{\text{Evaporation rate}}{v \cdot A} \tag{15}$$

N_t is calculable since all the terms on the right hand side of Eq (15) are known. It remains to determine S in Eq (14). A typical value for $V_c \Omega \varepsilon$ of 4.189×10^{-14} stern-m^3, as calculated by Kasper, completes the information needed to determine the expected number of fluorescent counts, D_f from Eq (14).

To find S, it is sufficient to know the Einstein coefficients for the transition $4p^1P_1 \longleftrightarrow 4s^1S_0$, the branching ratio, and the amount of time the atoms spend in the beam. There are sev-

eral energy levels between the $4p^1P_1$ state and the ground state. They are the $3d^1D_2$, $3d^3D_{1,2,3}$ and $4p^3P_{0,1,2}$ states. Examination of the Grotrian diagrams and a listing of observed transitions for calcium reveals that the $4p^1P_1$ state relaxes directly to the ground state with a branching ratio of 100% (Ref 26:340-358, 30:401-404). The branching ratio allows the transition $4s^1S_0 \leftrightarrow 4p^1P_1$ (4226 Å) to be modeled as a two level system (Figure 7). The average number of spontaneous emissions per atom per unit of time in the laser beam is

$$S = \frac{T_t \cdot \Gamma_p}{T_e} \tag{16}$$

where

S is the number of spontaneous emissions/atom

T_t is the total time the atom spends in the beam

Γ_p is the fraction of transitions that are spontaneous

T_e is the time for the atom to complete one transition cycle

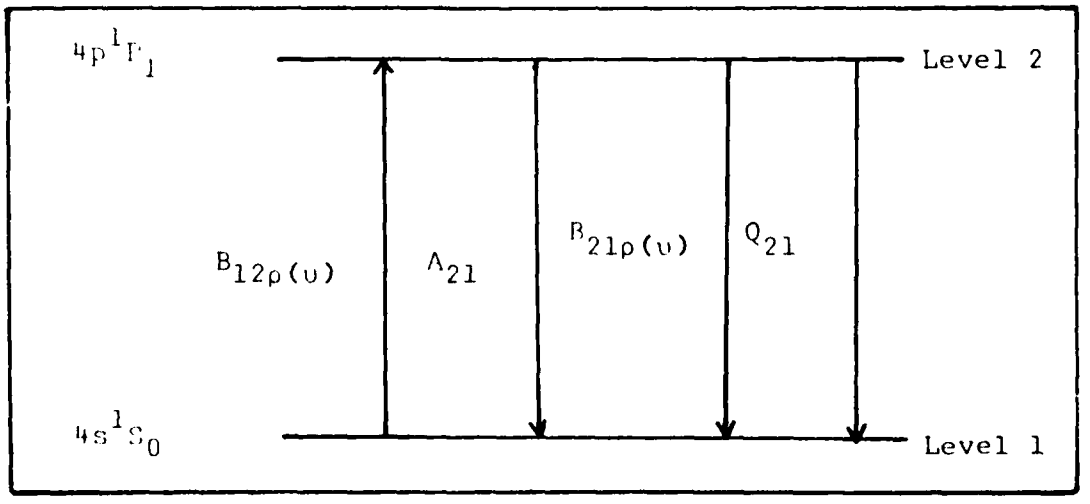

Figure 7. Two Level Model of Transition

Referring to Figure 7,

$$T_e = \frac{1}{A_{21}+B_{21}\rho(\upsilon)} + \frac{1}{B_{12}\,\rho(\upsilon)} \tag{17}$$

and

$$\Gamma_p = \frac{A_{21}}{A_{21}+B_{21}\rho(\upsilon)}$$

where

A_{21} is Einstein coefficient of spontaneous emission (sec^{-1})

$B_{21}\,\rho(\upsilon)$ is rate of stimulated emission (sec^{-1})

$B_{12}\,\rho(\upsilon)$ is the rate of absorption (sec^{-1})

$\rho\,(\upsilon)$ is the spectral energy density of the radiation field $(\frac{Joule}{m^3 hz})$

Quenching has been ignored because of the low pressure in the test cell. By use of the following relationships and knowledge of A_{21}, g_1, and g_2 for the transition (Ref 27:E-314),

$$\frac{A_{21}}{B_{21}} = \frac{8\pi h\upsilon^3}{c^3} \tag{19}$$

and

$$B_{12}g_1 = B_{21}g_2 \tag{20}$$

The values for B_{12} and B_{21} are found to be 9.88×10^{20} and 2.96×10^{21} $(\frac{m^3}{Joule\text{-}sec^2})$. The spectral energy density is

$$\rho(\upsilon) = \frac{P}{A\,\Delta\upsilon c} \tag{21}$$

where

P is incident laser power (watts)

A is beam cross sectional area (m^2)

$\Delta\upsilon$ is the laser line width (hz)

c is the speed of light (m/sec)

From experience, the apparatus has been found to deliver 50-100 mW to the test cell. Choosing the lower value to be conservative and using typical values of .5 mm for the beam diameter and 10 GHz for $\Delta\upsilon$, one finds $\rho(\upsilon)$ to be 8.5×10^{-14} $(\frac{\text{Joule-sec}}{m^3})$. The total time is just

$$T_t = \frac{\text{Beam diameter}}{V_{rms}} \qquad (22)$$

The Eqs (16)-(22) yield an approximate value of 94 for S. Evaluation of Eq (14) reveals that an expected fluorescent count rate of about 6×10^3 counts/sec would be detected under the operating conditions assumed.

The conclusion is that calcium detection would be feasible using this scheme. The extant apparatus would have to be modified slightly (Figure 8). The pump laser would have to be replaced with one capable of delivering 1.5 W at 351.1 and 363.8 nm since Stilbene 420 is the recommended dye for the dye laser. The PCA 8850 photomultiplier tube which has a spectral response of 260-660 nm could be retained.

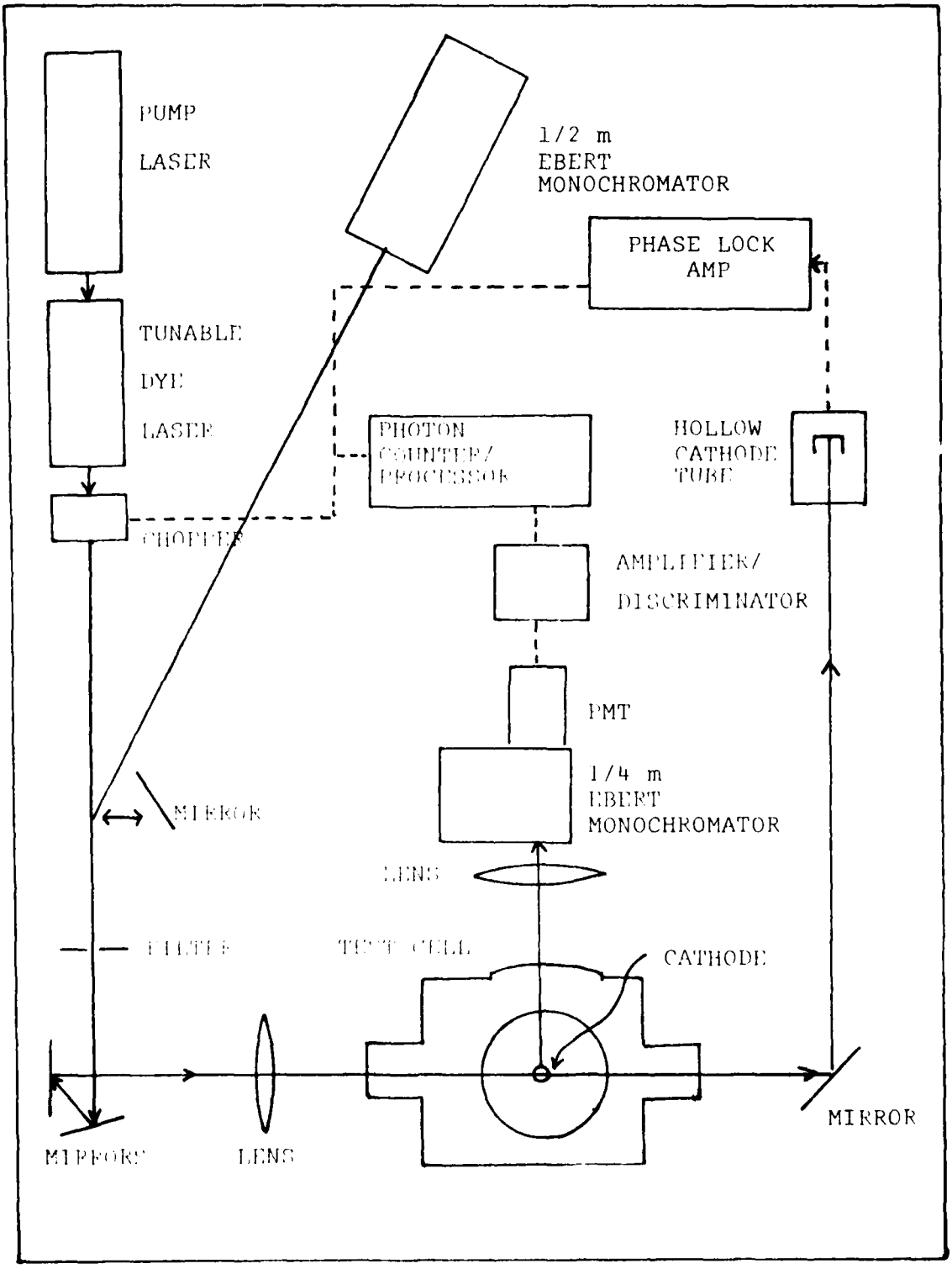

Figure 8. Apparatus to Detect Calcium -- Approach I

Description of Operation

A pump laser (351-363 nm and 1.5 W output) excites a tunable dye laser (Spectra Physics model 375) charged with Stilbene 420 dye. The dye laser is tuned roughly to 4226 Å by diverting the output beam into a 0.5 meter Ebert monochromator. Fine tuning to the atomic transition is accomplished and continuously monitored by the optogalvanic effect in the calcium hollow cathode tube. The gas discharge in the tube reaches a steady state unless disturbed by radiation of a wavelength matching an atomic transition of one of the gas species. The voltage across the gas discharge is monitored for the optogalvanic effect by a phase lock amplifier.

Once the laser beam is tuned to a resonance wavelength, it is focused by a lens and passed through the evacuated test cell parallel to the top of the cathode and perpendicular to the view port. Fluorescent radiation from the evaporant passes through the view port and is focused on the input slit of a 0.25 m Ebert monochromator. The monochromator is tuned to the resonance transition thus acting as a filter to background radiation.

The fluorescent radiation is then passed through the photon counting system which consists of the photomultiplier tube (RCA 8850), an amplifier/discriminator, and a photon counter/processor. The counting system is synchronized with a mechanical chopper which chops the laser beam before it enters the test cell. Chopping the beam allows for separation of the background from the signal by activation of two counters corresponding to the laser

on/laser off condition.

Approach II. Double Pumping of the Calcium Atoms

Although the $4s^1S_0 \leftrightarrow 4p^3P_1$ (6573 Å) transition is easily excited by a laser operating with R640 dye, the metastable nature of the upper state denies detection of calcium by monitoring fluorescence from the $4p^3P_1$ state. If, however, the atoms are double pumped from the $4p^3P_1$ state to another state which has a short lifetime, the fluorescence from the uppermost state could be monitored and related to the calcium evaporation rate. There are two simple ways to gain double pumping: one is to use a flash lamp to excite absorption from the $4p^3P_1$ state, and the second is to collinearly irradiate the atoms with a second laser beam of the desired wavelength. These two methods are precisely those

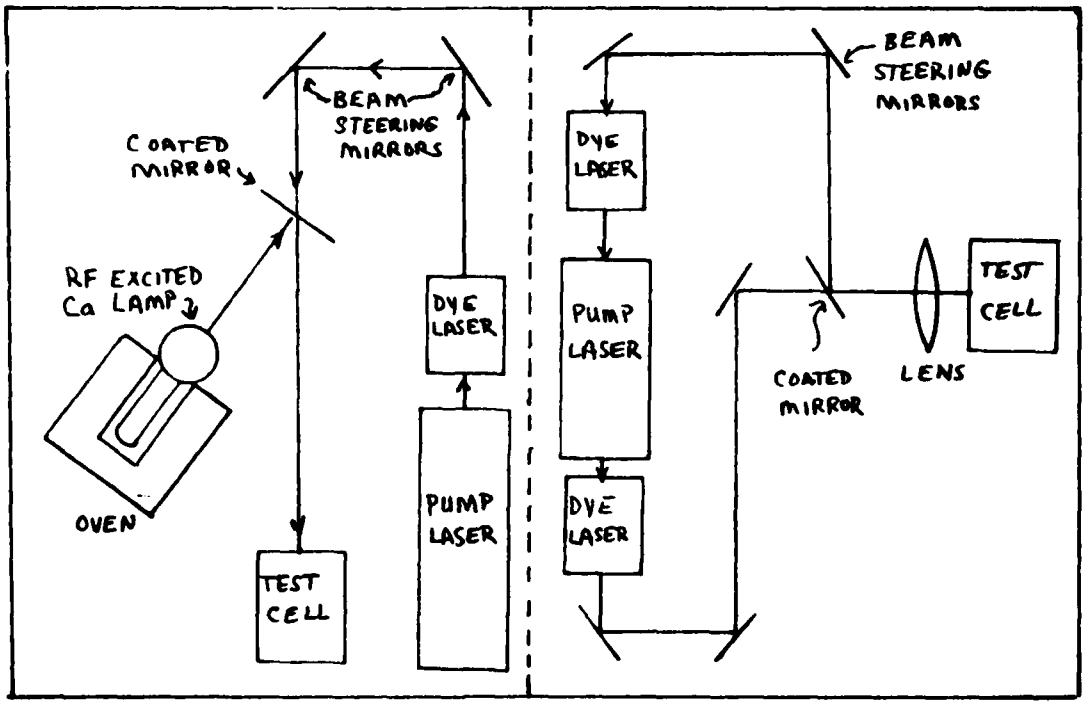

Figure 9. Illustration of Two Methods of Double Pumping

used by workers measuring the $4p^3P_1$ state lifetime (Ref 28:31). Figure 9 illustrates the two methods.

First the calcium atoms are pumped by a laser to the $4p^3P_1$ state and then to a second level. Obviously, there are three criteria relevant to the second level. The level must be separated from the $4p^3P_1$ state by an energy difference that is within dye laser range. The level should have a short lifetime (10^{-7} sec or shorter). Finally, the second level should relax by only one or at most two paths to lower levels. A perusal of references (26) and (30) leads to the two possibilities of $4p^3P_1 \leftrightarrow 5s^3S_1$ (6122 Å) and $4p^3P_1 \leftrightarrow 4d^3D_2$ (4435 Å). Baskin's Grotrian diagram also lists a $4p^3P_{0,1,2} \leftrightarrow 5s^1So$ (5581.97 Å) intercombination (Ref 26:358), but Striganov disagrees, listing it as $3d^3D_2 \leftrightarrow 4p'^3D_3^o$ (Ref 30:402). The lifetime for the $4d^3D_2$ state is 1.5 x 10^{-8} sec and for the $5s^3S_1$ is 3.5 x 10^{-8} sec (Ref 27:E-342). Both levels apparently relax to the $4d^3P_1$ state only and the $4d^3P_1$ state relaxes to the $4s^1So$ state only, thus simplifying the analysis considerably. This approach reduces to a three level model (Figure 10).

Since level 2 is metastable with a lifetime that is long compared to the time the atoms are in the laser beam, the three level model can be approximated as a two level model between levels 2 and 3. Then if similar calculations are made as for $4s^1S_0 \leftrightarrow 4p^1P_1$ (4226 Å) transition, the expected flourescent signal detected is about 1.3 x 10^3 counts/sec for the $4p^3P_1 \leftrightarrow 4d^3D_2$ (4435 Å) transition and 6 x 10^7 counts/sec for the $4p^3P_1 \leftrightarrow 5s^3S_1$

(6122 Å) transition. A $\rho'(\upsilon)$ of 8.5×10^{-14} $(\frac{\text{Joule}}{\text{m}^3\text{-HZ}})$ corresponding to a dye laser power output of 50 mW was assumed.

The conclusion is that this approach is feasible for the 4435 Å transition and unfeasible for the 6122 Å transition based upon the criteria developed earlier in the problem analysis section. Since the $4p^3P_1 \leftrightarrow 4d^3D_2$ transition would require the dye laser to incorporate Stilbene 420 dye, this approach has no advantages over the first considered.

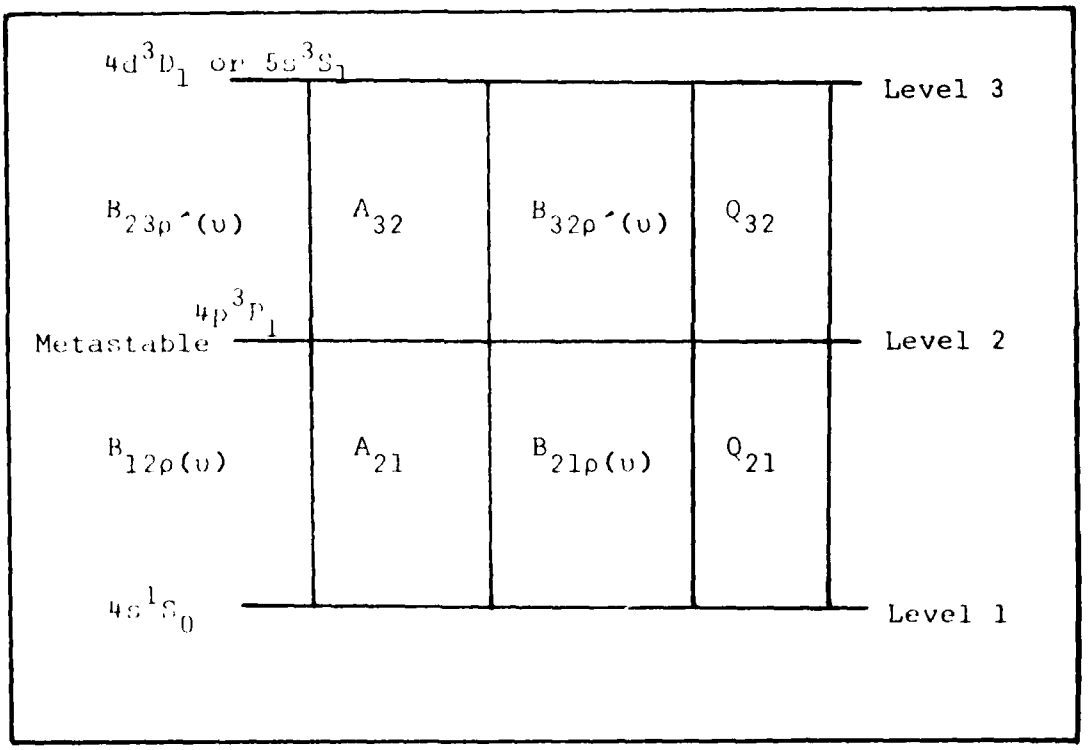

Figure 10. Three Level Model of Transition

Approach III. Ionization

Atoms can be ionized either by absorption of light quanta, field ionization, or inelastic collisions with electrons, neutral particles, or ions. Impact ionization requires elaborate apparatus to focus and ionize the atomic beam. Since the atomic beam must be dense to offset the sparsity of Ca atoms, impact ionization is not well suited to the problem. A dense beam could scatter and erode the cathode surface. Field ionization was not investigated because of time constraints. The remaining option is ionization by light quanta.

Excited atoms are easier to ionize than those in the ground state. Since the first ionization energy of calcium is 6.11 eV, excitation of the atoms is necessary to achieve ionization by absorption of light quanta. Unfortunately, the calcium atoms do not leave the cathode in an excited state. Comparison of the number of atoms in the lowest excited state to the ground state at the cathode operating temperature (1050° C) gives

$$\frac{n_1}{n_0} = \frac{e^{-E_1/kT}}{e^{-E_0/kT}} \sim 10^{-11} \qquad (23)$$

If the calcium atoms are excited by a laser beam before being ionized by further absorption of light quanta, the task is made easier (Figure 11). Excitation to a metastable level is preferable so that losses from the excited level to ground state are negligible over the time span the atoms are in the beam. Ionization of calcium from the $4p^1P_1$ state requires light of 3904 Å and from the $4p^3P_1$ state light of 2935 Å. Incandescent lamps,

enclosed low pressure arcs, and metallic arcs with incandescent electrode are all sources of continuous spectra in the near ultraviolet range (Ref 33:166-198). Figure 12 delineates an experimental setup.

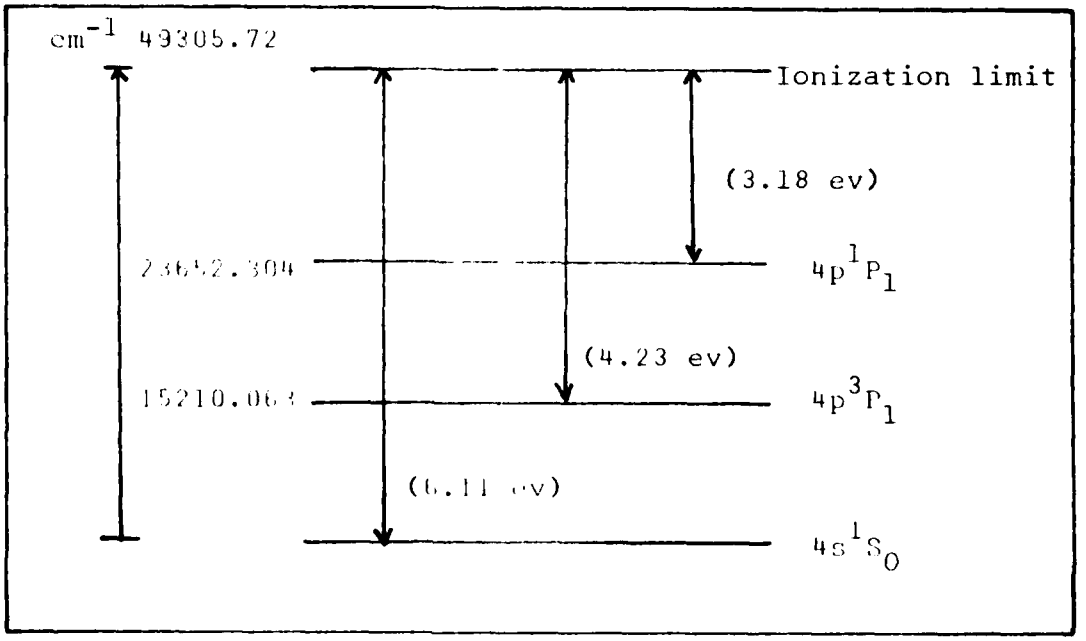

Figure 11. Ionization Limit of Calcium

The maximum signal that such a configuration could produce is

$$I = f_i f_c \frac{F_c \cdot e}{t} \tag{24}$$

where

t is the time of charge collection (sec)

F_c is number of Ca atoms entering ionization volume (atoms/sec)

e is the fundamental electric charge (1.6×10^{-19}coul)

f_i is fraction of Ca atoms ionized

f_c is fraction of electrons collected

If all the atoms were ionized, all the resultant electrons were collected, and there were no leakage of cathode produced electrons past the negative plate at the ionization volume boundary, the maximum signal is 4.3×10^{-10} Amps for 2.7×10^{9} atoms/sec being ionized. Of course f_i and f_c are not ever going to be unity. However, pico coulomb currents are measurable. Conservatively, if only 1% of the atoms are ionized and 10% of those are collected, the current would be measurable.

The conclusion is that detection of calcium atoms by ionization is feasible. Practical considerations could become a problem though. Introduction of charged plates to collect the ionization current could have an unknown effect on the evaporation characteristics of the cathode. This method should be considered only if the first approach discussed cannot be made to work.

Description of Operation

The pump laser excites the dye laser which is tuned to 6573 Å. The dye laser beam is focused above the cathode, exciting the evaporating Ca atoms to the $4p^3P_1$ metastable state. The excited atoms pass through the slit in the lower electrode which is negatively charged to deflect the cathode emission current. A UV light source with a component at 2935 Å in synchronization with the chopper open interval is focused into the volume between the electrodes. The excited Ca atoms are ionized and the ioniza-

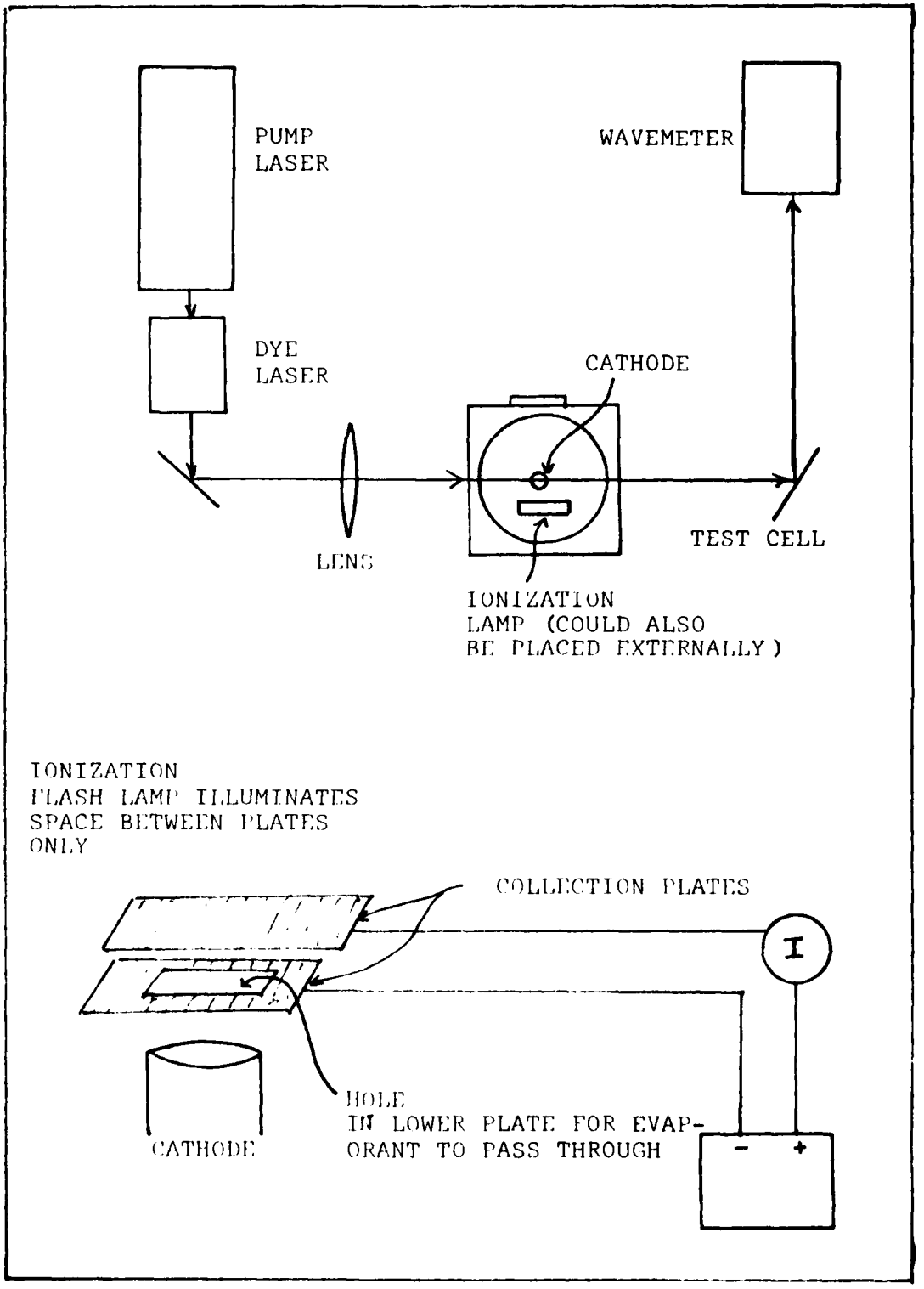

Figure 12. Ionization Apparatus

tion current is collected by the positively charged upper electrode. If the view port is constructed of material transparent to the UV spectrum, the light source could be external to the test cell.

Other Methods Considered

Sensitized fluorescence and stimulated emission were considered and discarded as viable methods of detecting and measuring calcium evaporation rates. Sensitized fluorescence occurs in gases and liquids when excited atoms of one type (donor atoms) transfer the excitation energy to atoms of another type (acceptor atoms). The transfer of energy occurs only if the acceptor atom has an unoccupied electron energy level of near resonance to that of the donor atom. Thus, in principle, calcium could be excited to the $4p^3P_1$ state, transfer its excitation energy to an acceptor atom's short lived level, and the resultant fluorescence measured. There are three compelling reasons why sensitized fluorescence is not suitable to the problem:

(1) Poisoning or ion sputtering of the cathode by acceptor gas (Ref 34:57).

(2) Acceptor gas pressure would have to be on the order of mTorr for the probability energy transfer to be significant.

(3) Calculating the event cross section and energy transfer rate falls into the category of quantum mechanical "hard problem". It is doubtful that a quantitative relation between the sensitized fluorescence intensity and calcium evaporation rates could be derived.

Boosting the stimulated emission rate from the $4p^3P_1$ state was also considered. Enhancement of the stimulated emission rate above the natural rate requires population inversion. Population inversion cannot be accomplished via a two step pumping scheme such as the $4s^1S_0 \longleftrightarrow 4p^3P_1$ transition. The calcium electronic structure does not lend itself to the ideal three or four step pumping scheme (Figure 13).

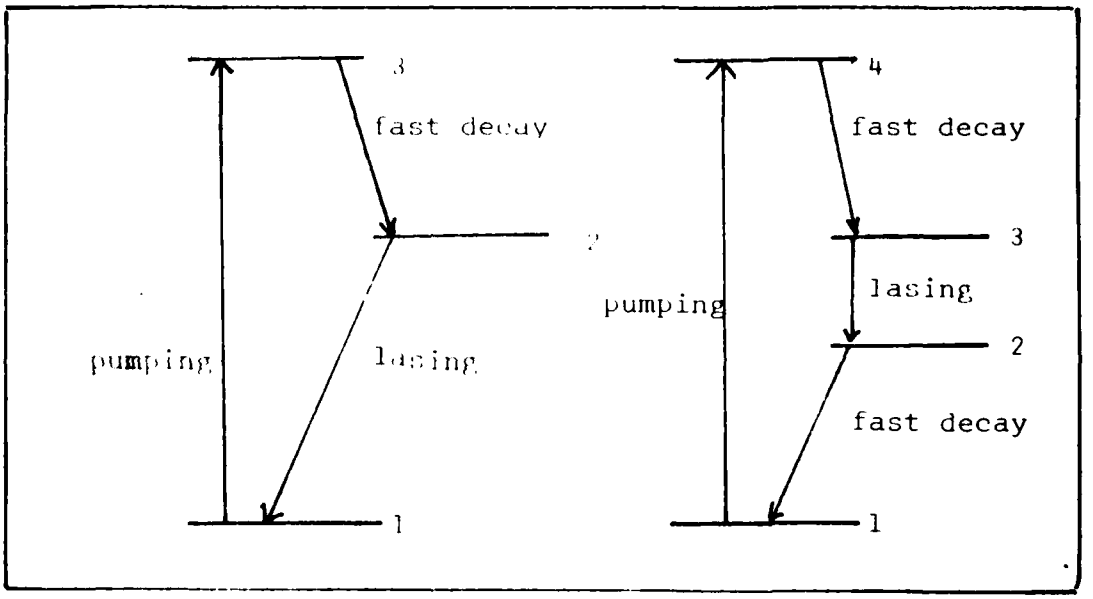

Figure 13. Ideal Pumping Schemes for Inversion (Ref 37:10)

Wavelength Calibration

All of the methods discussed require setting a laser at a specific wavelength. Tuning the laser via the optogalvanic effect is only applicable for 4226 Å because that is the only calcium transition the calcium hollow cathode tube responds to.

Tuning to the 6573 Å, 6122 Å or 4435 Å transitions must be accomplished in some other way.

Most modern wavemeters employ interferometry to measure wavelength. Other methods measure the absolute frequency of the laser from which the wavelength is obtained by the relationship c/υ (Ref 35:189-195). Hänsch has devised a self-calibrating grating for wavelength measurement which is superior to conventional interferometric methods (Ref 36:423). In future experiments involving laser induced fluorescence where the optogalvanic effect is not suitable for measuring the laser wavelength, Hänsch's method could be employed.

III. Direction of Future Experiments

The ultimate goal of using laser induced fluorescence to study the behavior of cathode evaporants is to gather enough significant data to construct a model of cathode physics. Perhaps lifetime studies of evaporants may not contribute as greatly to the goal as first envisioned. Lifetime studies of evaporation rates are not amenable to being conducted in a thesis quarter because of time constraints. Accelerated lifetime tests are hampered by early heater filament degradation and failure. The filament emissions from overheated cathodes also coat and block the view port. More ominous is the lack of correlation between evaporant behaviors reported by various researchers. For instance, one researcher reported a $t^{-0.5}$ decrease in evaporation rate (Ref 14:154) while another doing an accelerated test reported a constant evaporation rate (Ref 13:170). It is likely that the evaporation rate is a complicated function of temperature and no one funtional relationship describes evaporation rate as a function of time for all temperatures.

Before any further attempts are made to quantify calcium evaporation rates, it must be ascertained that calcium does indeed evaporate from the cathode. The preponderance of experimental evidence indicates that calcium does evaporate from modern cathodes (Ref 14, 15) despite the perplexing absence of calcium in the evaporant stream reported by one researcher (Ref 11:255). A Varian Partial Pressure Gauge (PPG) operated in the mass spectrometer mode and mounted to intercept the evaporant stream could provide a de-

tection capability for calcium with a 10^{-12} Torr sensitivity (i.e., about 8 x 10^{8} Ca atoms in a volume of .025m^3 at 293 K). Also, the evaporant that plates out on the cold finger could be chemically analyzed for calcium. It would be necessary to ensure that any calcium deposited was not solely the result of surface detritus left on the cathode surface from the manufacturing process.

The test cell configuration presently includes a PPG which is mounted about 12 inches to one side of the cathode. There are two 90° bends in the 1 inch tubing which connects the point of PPG access to the evacuated volume and the test cell containing the cathode. Geometry renders it unlikely that any Ca gas will negotiate the tubing to reach the PPG. Nevertheless, a number of mass spectra were taken with the cathode operating at different temperatures. Residual atomospheric gases limited the PPG sensitivity to 10^{-9} Torr. Calcium was not observed in the mass spectra.

Rather than pursuing accelerated lifetime tests, it might prove more fruitful to examine evaporation rates as a function of temperature and then try to fit these rates to models of additive movement within the cathode based upon Knudsen flow, diffusion, and migration. An interesting phenomenon involving an increase in evaporation rate until 1200° K was reached, followed by a decrease of evaporation rate, was observed by Kasper (Ref 23:48). Appendix A details some further experiments to characterize this phenomenon. Modeling of the evaporation rate as a

function of temperature might also be useful in answering the following questions:

(1) Does the additive evaporate from the surface, the pores, or both?

(2) If it evaporates from the surface, how is the monolayer replenished?

(3) What is the replenishment rate to the surface dependent on?

IV. Conclusions and Recommendations

Conclusions

Three methods of detecting and measuring calcium evaporation rates were explored. Laser induced resonance fluorescence of the $4s\,^1S_0 \leftrightarrow 4p\,^1P_1$ (4226 Å) transition appears to be feasible and the easiest to implement. Double pumping of the calcium atoms from the $^3P_1$ state to a state of shorter lifetime is feasible for the $4p\,^3P_1 \leftrightarrow 4d\,^3D_2$ transition, but nothing is gained in case of experimental technique over the $4s\,^1S_0 \leftrightarrow 4p\,^1P_1$ transition. Ionization of the calcium atoms and measurement of the ion current is feasible but would require significant alteration of the apparatus and an alternative to the optogalvanic effect for tuning the laser. It has no advantages over the resonance fluorescence approach. The resonance fluorescence approach requires only that the pump laser be changed since the present argon pump laser can deliver a maximum of 60 mW of power to the dye laser at the necessary wavelengths.

Recommendations

The following recommendations are offered:

(1) Ascertain that calcium is evaporating from the cathode by use of a HPC operating in the mass spectrometer mode or by chemical analysis.

(2) Cease lifetime studies and concentrate on understanding the temperature dependence of the evaporation rate of barium and calcium.

(3) Model the mechanism by which barium/calcium reach the

cathode surface.

(4) Use Green's model to calculate the expected decrease in work function and compare with experimental results (Ref 20).

(5) Redesign the bellows adjustment mechanism that controls the cathode placement. The present mechanism is wobbly and difficult to work with.

(6) Design a stable, adjustable mount for the detection optics. The adjustment controls should be calibrated so that positioning is reproducible.

Bibliography

1. Stupian, G. W. A Review of the Science and Technology of Cathodes From the Viewpoint of Spacecraft TWT Applications. SD-TR-80-37. Los Angeles AFS, California: Space Division, June 1970 (AD A085778).

2. Cronin, J. L. "Modern Dispenser Cathodes," IEEE Proceedings Part I, 128 (1): 19-32 (February 1981).

3. Technical Bulletin: Semicon Dispenser Cathodes. Semicon Associates, Inc., Lexington, KY.

4. Forman, R. "Surface Studies of Barium and Barium Oxide on Tungsten and Its Application to Understanding the Mechanism of Operation of an Impregnated Tungsten Cathode," Journal of Applied Physics, 47 (12): 5272-5279 (December 1976).

5. Forman, R. "Use of Auger Spectroscopy in the Evaluation of Thermionic Cathodes," IEEE Transactions Electronic Devices, 24 (1): 56-61 (January 1977).

6. Forman, R. "Proposed Physical Model for the Impregnated Tungsten Cathode Based on Auger Surface Studies of the Ba-O-W System," Applications of Surface Science, 2 (2): 258-274 (January 1979).

7. Kittner, E. S., R. H. Ahlert, and W. C. Rutledge. "Studies on the Mechanism of Operation of the L Cathode I," Journal of Applied Physics, 28 (2): 156-166 (February 1957).

8. Kittner, E. S., W. C. Rutledge, R. H. Ahlert. "On the Mechanism of Operation of the Barium Aluminate Impregnated Cathode," Journal of Applied Physics, 28 (12): 1468-1473 (December 1957).

9. Kittner, E. S. "On the Mechanism of Operation of the Type B Impregnated Cathode," Journal of Applied Physics, 48 (10): 4344-4346 (October 1977).

10. Baun, W. L. "Characterization of Tungsten Impregnated Dispenser Cathode Using ISS and SIMS," Applications of Surface Science, 4 (3-4): 374-384 (April 1980).

11. Jones, D., D. McNeely, and L. W. Swanson. "Surface and Emission Characterization of the Impregnated Dispenser Cathode," Applications of Surface Science, 2 (2): 232-257 (January 1979).

12. Strauss, F., J. Bretting, and E. Metivier. "Traveling Wave Tubes for Communication Satellites," Proceedings of the IEEE, 65 (3): 387-400 (March 1977).

13. Rutledge, W. C. and E. S. Rittner. "Studies on the Mechanism of Operation of the L Cathode II," Journal of Applied Physics, 28 (2): 167-173 (February 1979).

14. Brodie, I., R. O. Jenkins and W. G. Trodden. "Evaporation of Barium from Cathodes Impregnated with Barium-Calcium-Aluminate," Journal of Electronics and Control, 6: 149-161 (February 1959).

15. Palluel, P. and A. M. Shnoff. "Experimental Study of Impregnated Cathode Behavior, Emission, and Life," Journal of Applied Physics, 51 (5): 2894-2902 (May 1980).

16. Maloney, C. E., C. R. K. Marian and G. Wyss. "Some Observations of Impregnated Tungsten Cathodes," Applications of Surface Science, 2 (2): 284-292 (January 1979).

17. Sickafus, E. N., M. A. Smith, J. S. Hammond, B. E. Artz and J. L. Bomback. "Surface Phenomena of Potential Concern to Longevity of Dispenser Cathodes," Applications of Surface Science, 2 (2): 213-231 (January 1979).

18. Rutledge, W. C., Milch, A., Rittner, E. S. "Measurement of Instantaneous Absolute Barium Evaporation Rates from Dispenser Cathodes," Journal of Applied Physics, 29 (5): 834-839 (1958).

19. Levi, R. "New Dispenser Type Thermionic Cathode," Journal of Applied Physics, 24: 233 (1953).

20. Green, M. Dispenser Cathode Physics. RADC-TR-81-211. Griffiss AFB, New York: Rome Air Development Center, July 1981 (AD A105126).

21. Jenkins, R. O. "A Review of Thermionic Cathodes," Vacuum, 19 (8): 353-359 (August 1969).

22. Zemyan, S. M. "Laser Induced Fluorescence of Barium Evaporating From a Dispenser Cathode," Unpublished MS thesis. School of Engineering, Air Force Institute of Technology, WPAFB, Ohio, March 1982.

23. Kasper, R. F. "Measurement of Barium Evaporation From a Dispenser Cathode Using Laser-Induced Fluorescence," Unpublished MS thesis. School of Engineering, Air Force Institute of Technology, WPAFB, Ohio, December 1982.

24. Fairbank, Jr. W. M., T. W. Hänsch and A. L. Schawlow. "Absolute Measurement of Very Low Sodium-Vapor Densities Using Laser Resonance Fluorescence," Journal of the Optical Society of America, 65 (2): 199-204 (February 1975).

25. Benham, V. N. "Sodium Concentration Measurement Using Laser Induced Fluorescence," Unpublished MS thesis. School of Engineering, Air Force Institute of Technology, WPAFB, Ohio, December 1981.

26. Bashkin, S. and J. O. Stoner, Jr. Atomic Energy-Level and Grotian Diagrams. Amsterdam-Oxford-New York: North-Holland Publishing Company, 1978.

27. Weast, R. C. and M. J. Astle. CRC Handbook of Chemistry and Physics (63rd edition). Boca Raton: CRC Press, Inc., 1982.

28. Furcinitti, P. S., L. C. Balling and J. J. Wright. "A Measurement of the $^3P_1$ Metastable State in Ca," Physics Letters, 53A: 75-76 (May 1975).

29. Model 375 Dye Laser With Model 376 or 376B Dye Circulator Instruction Manual With Proc/Spec Sheet. Mountain View, California: Spectra Physics, Inc., 1980.

30. Striganov, A. R. and N. S. Sventitskii. Tables of Spectral Lines of Neutral and Ionized Atoms. New York-Washington: IFI/Plenum, 1968.

31. Havey, M. D., L. C. Balling and J. J. Wright. "Direct Measurements of Excited-State Lifetimes in Mg, Ca, Sr," Journal of the Optical Society of America, 67 (4): 488-491 (April 1977).

32. Vályi, L. Atom and Ion Sources. London-New York-Sydney-Toronto: John Wiley and Sons, 1977.

33. Harrison, G. R., R. C. Lord and J. R. Loofbourow. Practical Spectroscopy. New York: Prentice-Hall, Inc., 1948.

34. Cronin, J. L. "Practical Aspects of Modern Dispenser Cathodes," Microwave Journal, 22 (9): 57-62 (September 1979).

35. Demtröder, W. Laser Spectroscopy Basic Concepts and Instrumentation V. New York: Springer-Verlag Berlin Heidelberg, 1981.

36. Hänsch, T. W. "A Self-Calibrating Grating" in Laser Spectroscopy III, edited by J. L. Hall and J. L. Carlsten. New York: Springer-Verlag Berlin Heidelberg, 1981.

37. Svelto, O. Principles of Lasers. New York-London: Plenum Press, 1976.

38. Model 1121A Amplifier-Discriminator Operating and Service Manual. Princeton, New Jersey: EG & G Princeton Applied Research, Inc., 1976.

39. Model 1112 Photon Counter/Processor Operating and Service Manual. Princeton, New Jersey: EG & G Princeton Applied Research, Inc., 1976.

APPENDIX A

Investigation of Evaporation Rate Phenomenon Reported by Kasper

Kasper measured a barium evaporation rate that increased with temperature until a peak was reached at about 1200° K, subsequently decreasing with increasing cathode temperature (Ref 23:38). Zemyan's data spanned 900-1050° K and thus does not corroborate Kasper's observation (Ref 22:51). Is the phenomenon noted by Kasper a result of cathode physics or is it a function of the photon counting system?

The photon counting system used by Kasper consists of an RCA 8850 photomultiplier tube (PMT), an EG&G Princeton Applied Research model 1121A amplifier-discriminator, and an EG&G Princeton Applied Research model 1112 photon counter/processor (Figure A-1).

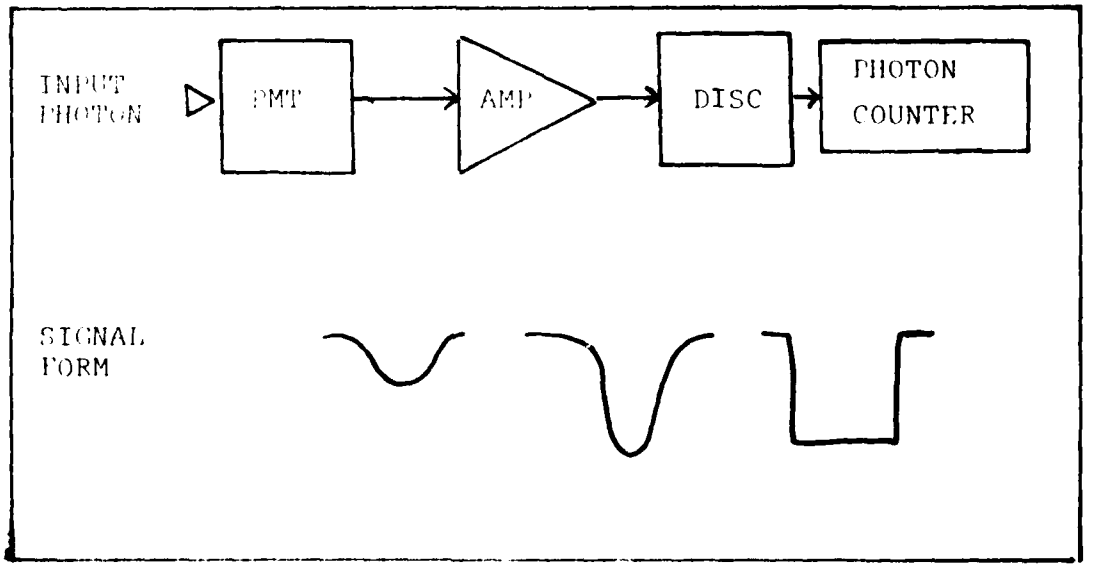

Figure A-1. Schematic of Photon Counting System (Ref 38:II-2)

The maximum number of events the system can count per second depends upon the dead time, resolving time, and the response characteristic (paralyzable or nonparalyzable) of the PMT and discriminator. The photon counter is also limited to a maximum data count of 99999999 per interval of measurement time. Any counts exceeding the limit are lost. The PMT is a paralyzable counter while the discriminator is nonparalyzable. The difference between a paralyzable and nonparalyzable counter is that the dead time increases with increasing input rate for the former and is a constant value independent of the input rate for the latter. Dead time is the interval during which the counter cannot recognize another pulse because it has been desensitized by the previous pulse. Resolving time is a measure of how close together two events can occur and still be distinguishable as separate events by the counter. When the input pulse rate exceeds the resolving time of the counter, pulse pile up error occurs. The counter adds the pulses it sees within the resolving time interval into one pulse. While the counter is processing one pulse, it cannot detect another incoming pulse and hence is "dead". Figure A-2 displays the relationship of input pulse rate to output pulses counted for paralyzable and nonparalyzable counters.

Since the resolving time of typical PMTs is 10-40 ns, pulse pile up error in the PMT would be observable in the range of 2.5×10^7 to 1×10^8 input pulses/sec. Kasper's laboratory notebook indicates that he had to operate the discrimator in the PRESCALE mode which means that there was a pulse pile up error exceeding

1% (Ref 39:IV-8). The evaporation vs temperature curve reported by Kasper looks suspiciously like the result of the PMT operating in the paralyzed region. An experiment was conducted to test the photon counting system.

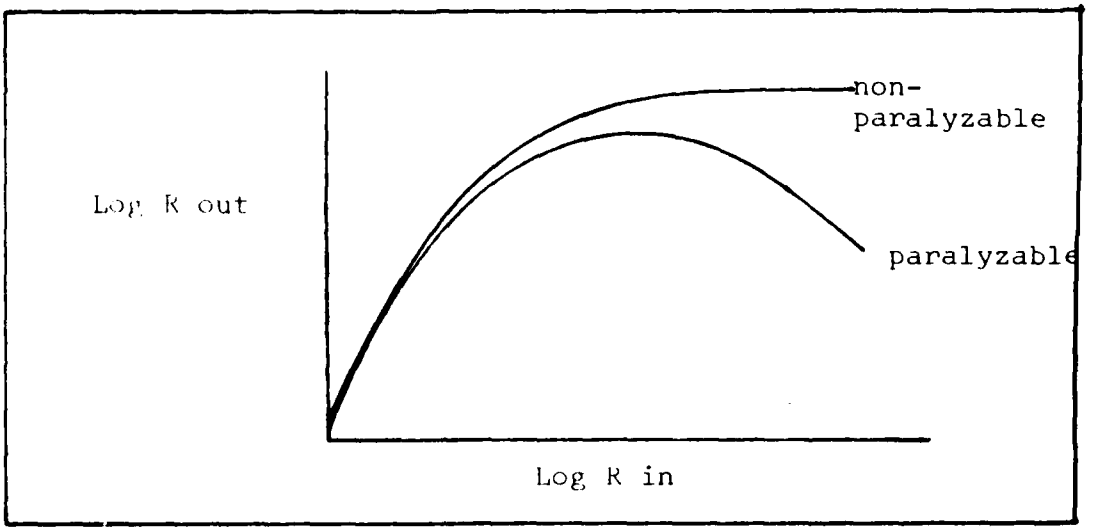

Figure A-2. Paralyzable-Nonparalyzable Response (Ref 39:IV-8)

Experimental Procedure

Measure the evaporation rate of barium vs cathode temperature at different incident laser powers. Graph the fluorescent count rate vs temperature for different laser power. The author used an SLFV cathode while Kasper and Zemyan used a type B cathode. If the evaporation curve reported by Kasper is a result of cathode physics, one would expect a set of curves similar to Figure A-3a. If the phenomenon is a function of pulse pile up error in the counting system, one would expect a set of curves similar to Figure A-3b. There is one other behavior (Figure A-3c) which could be expected as a result of saturation of the fluorescent transi-

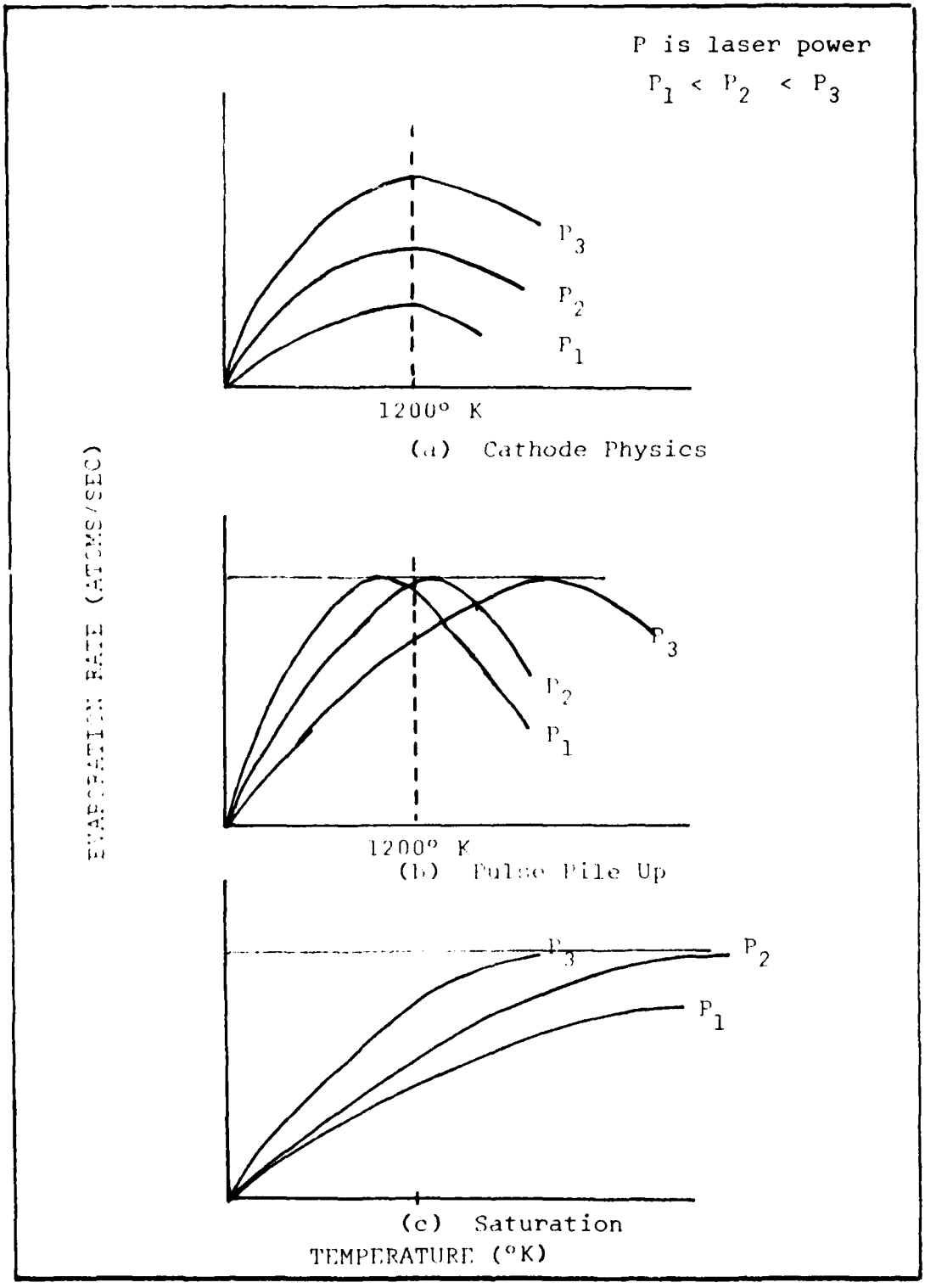

Figure A-3. Possible Evaporation Vs Temperature Curves

tion. Since the evaporation rate of barium cannot exceed the replenishment rate to the surface from the reservoir, there is conceivably an upper limit to the evaporation rate as the temperature increases. Also, for any specific incident laser power the fluorescing transition saturates and the signal should approach some constant value.

Two sets of experimental data were taken. The first (shown in Figure A-4) corresponds to Figure A-3a in that the peak relative evaporation rates for each laser power occur at the same temperature, in this instance 1050° K instead of 1200° K as Kasper found. There are several oddities not observed by Kasper, specifically, the dip at 1000° K and the plateau between 1150 and 1250° K for the lower laser powers with a corresponding second peak for the higher powers in the same temperature range (Figure A-4). Note also the inversion of the 100 mW curve with the 80mW curve which may be caused by the mode structure of the dye laser at 100 mW. The two curves at 100 and 135 mW are suspect. The net fluorescent counts at 100 and 135 mW are based on interpolated scattering counts at those powers. Actual scattering counts for 100 and 135 mW were not taken because of pump laser instability. The laser was stable for the duration of measurements at 50, 63, and 80 mW.

The second set of data was taken a few days after the first to corroborate the first. Unfortunately, the detection optics had been jarred enough to make detection of fluorescence impossible. After realignment of the detection optics, data was

taken and the resultant curve at 50 mW appears to follow the behavior noted by Kasper with the exception of the peak being shifted from 1200 to 1000° K (Figure A-5). The experiment was terminated at 1150° K during taking of the second set of data because the pump laser failed. Data for 1100° K was not included because of pump laser instability during the measurements. Note that the 100 mW curve lies below the 80 mW curve again.

The graphs in Figures A-4 and A-5 are of relative evaporation rates. That is, Zemyan's basic equation (Ref 22:21):

$$N_t = \frac{(.7)8\pi^2}{99} \frac{P_f}{h\upsilon} \frac{D}{v} \frac{1}{\Omega\varepsilon V_c} \qquad \text{(A-1)}$$

where the quantities are the same as noted after Eq (14) in the main body of this paper, was rewritten in the form

$$N_t vA\ (\Omega\varepsilon V_c) = \frac{(.7)8\pi^2}{99} \frac{(\#\ \text{fluorescent counts} \cdot h)_D}{h\upsilon} \cdot A \qquad \text{(A-2)}$$

The left hand side of (A-2) is the evaporation rate times a constant. Expressing (A-1) in this manner precludes the necessity of conducting Rayleigh scattering on N_2 in the test cell to determine $\Omega\varepsilon V_c$. The obvious advantages are that it saves time and saves exposure of the cathode to atmospheric pressure. If a standard $\Omega\varepsilon V_c$ is chosen, then all sets of data can be normalized to the same value and readily compared.

Discussion of Results

Clearly the data taken thus far is not conclusive. It is not certain that the second data follows the trend of the first

because the experiment was terminated early by pump laser failure. However, the lack of a definite peak at 1050° K suggests the curve shapes of the first data set are not being duplicated in the second data set. The realignment of optics between the taking of the first data set and the second should have changed the magnitude of the relative evaporation rates but not the curve shapes. The graphs of the second data set (Figure A-5) resemble a graph of scattered counts vs laser power for different temperatures (Ref 22:47) and the two could easily be confused. However, if the raw data of the second set is plotted as gross scattered counts vs laser power, a different family of curves is obtained and it becomes clear that the two graphs have nothing in common. (Figure A-6). The absence of a shift in peaks to lower temperature as laser power increases for both data sets strongly suggests that pulse pile up error is not the cause for the phenomenon.

The exclusion of pulse pile up error as the cause for the phenomenon does not preclude some unknown peculiarity of the photon counting system from being the cause. It is odd that the barium evaporation rate in all the experiments peaks before the cathode operating temperature is reached (1050° C or 1323° K). There is another oddity that should be mentioned here. Zemyan tuned the laser off the resonance wavelength, precluding excitation of barium fluorescence, and measured the laser scatter from the vapor. If the evaporation rate is changing with temperature, one would expect the laser scatter from the vapor to track the change in

the evaporation. In fact, Zemyan could discern no difference as the cathode temperature varied. Either the change in laser scatter from the vapor was too insignificant to be separable from the laser scatter from the test cell or the barium evaporation rate did not change significantly as the cathode temperature was varied. The latter speculation is in direct conflict with Kasper's experimental results. The experimental evidence collected thus far is not conclusive enough to attribute the phenomenon to a cause.

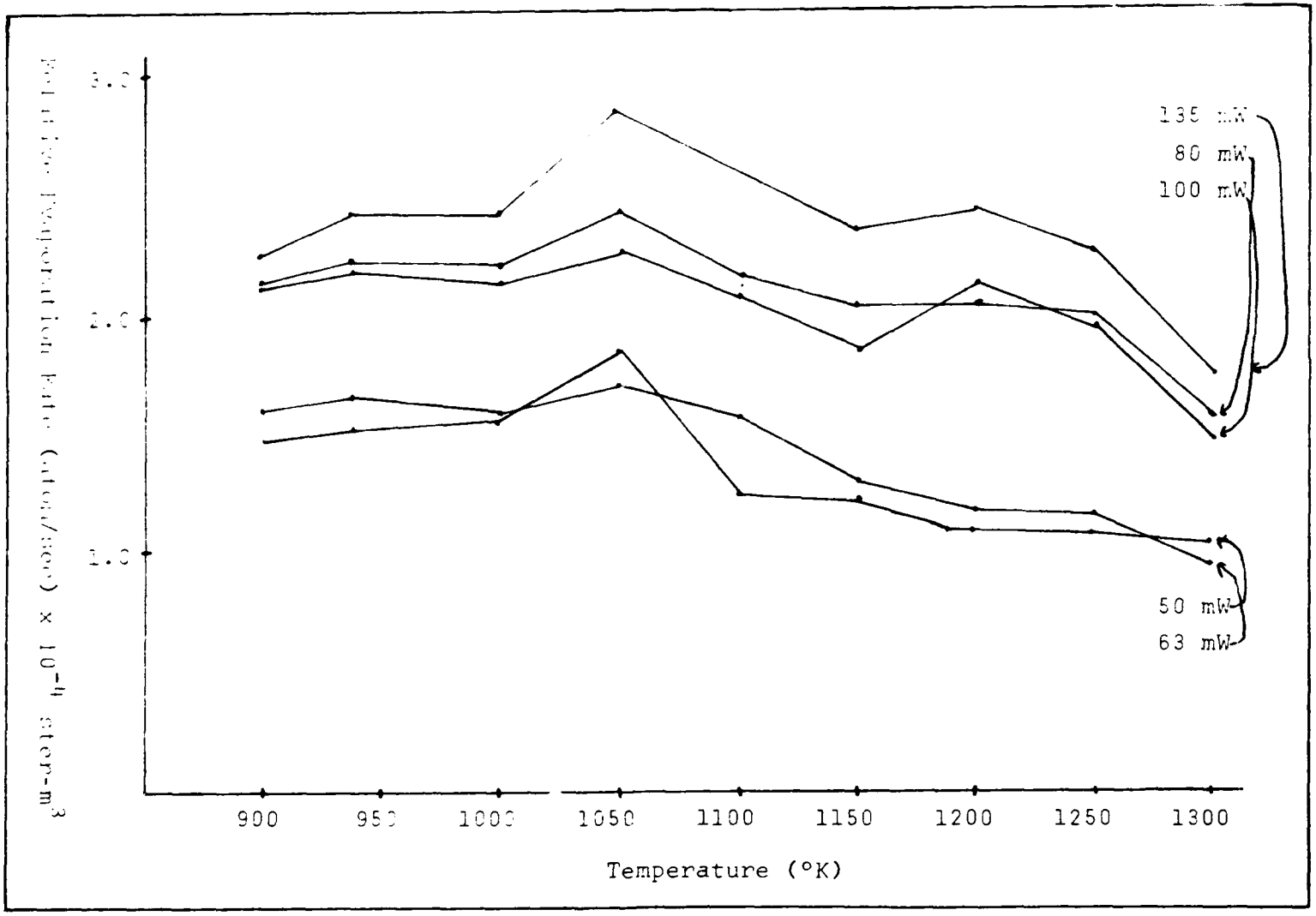

Figure A-4. Relative Evaporation Rate Vs Temperature (first data set)

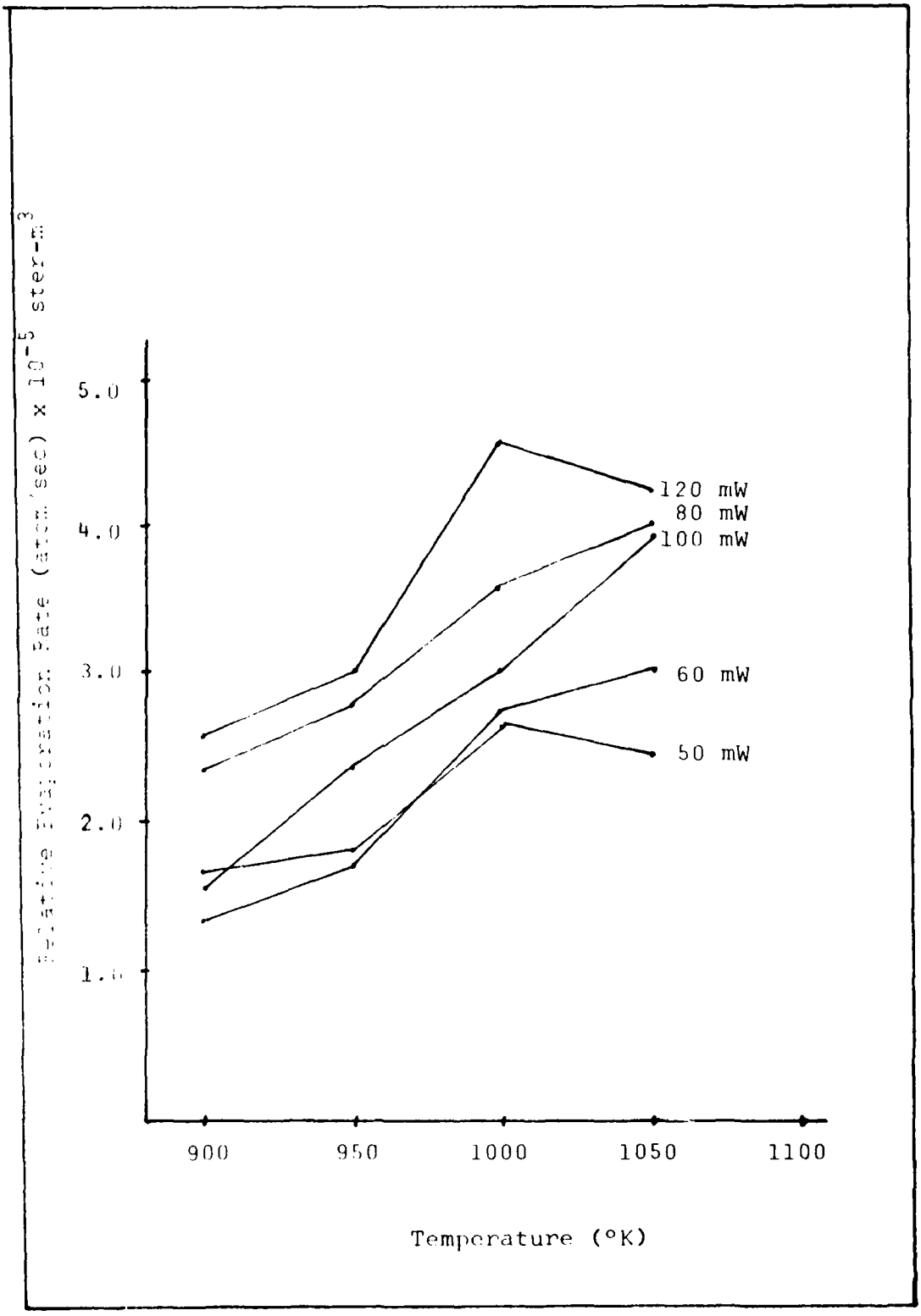

Figure A-5. Relative Evaporation Rate Vs Temperature (second data set)

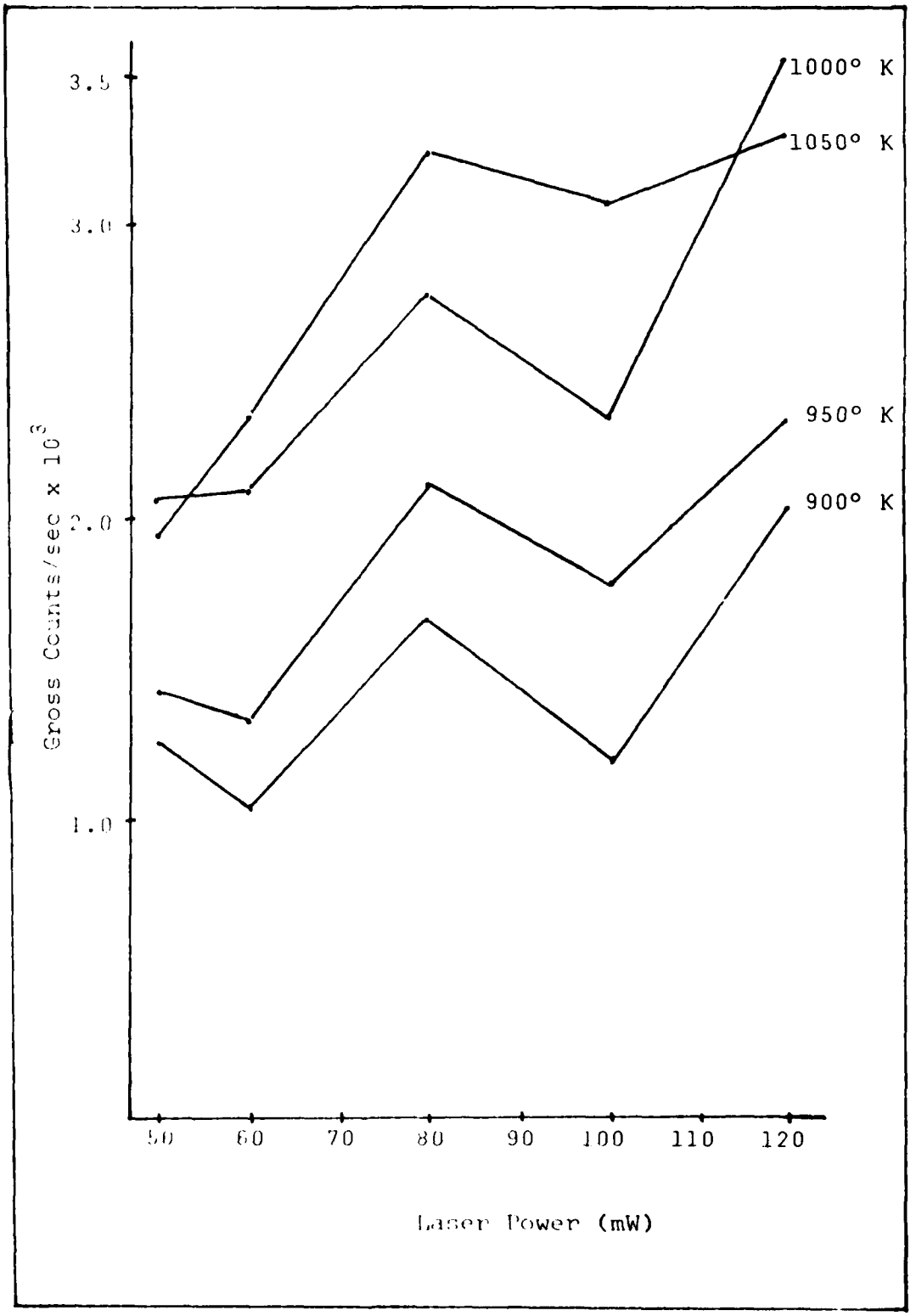

Figure A-6. Gross Counts Vs Laser Power for Different Temperatures

VITA

Virginia Louise Eason was born on 9 May 1949 in New Orleans, Louisiana. She graduated from high school in Jackson, Mississippi, in 1967 and attended Louisiana State University, Baton Rouge, Louisiana, from which she received the degree Bachelor of Science in Physics in May 1972. After graduation, she was employed for 2 1/2 years by the Physics Department of Louisiana State University where she worked with Dr. W. O. Hamilton on a project to detect gravity waves. She worked for a short period as an instrument technician at the Exxon Oil Refinery in Baton Rouge, Louisiana. She joined the U. S. Navy in May 1974 and was employed in operations at Naval Facilities Keflavik, Iceland; Argentia, Newfoundland; and Centerville Beach, California; before entering the School of Engineering, Air Force Institute of Technology, in June 1981.

SECURITY CLASSIFICATION OF THIS PAGE (When Data Entered)

REPORT DOCUMENTATION PAGE		READ INSTRUCTIONS BEFORE COMPLETING FORM
1. REPORT NUMBER AFIT/GNE/PH/83M-6	2. GOVT ACCESSION NO. AD-A127357	3. RECIPIENT'S CATALOG NUMBER
4. TITLE (and Subtitle) EXAMINATION OF THE FEASIBILITY OF DETECTION OF CALCIUM EVAPORATION FROM A TYPE B DISPENSER CATHODE BY LASER INDUCED PHENOMENA		5. TYPE OF REPORT & PERIOD COVERED MS THESIS 6. PERFORMING ORG. REPORT NUMBER
7. AUTHOR(s) Virginia L. Eason Lt, USN		8. CONTRACT OR GRANT NUMBER(s)
9. PERFORMING ORGANIZATION NAME AND ADDRESS AIR FORCE INSTITUTE OF TECHNOLOGY (AFIT-EN) WRIGHT-PATTERSON AFB , OHIO 45433		10. PROGRAM ELEMENT, PROJECT, TASK AREA & WORK UNIT NUMBERS
11. CONTROLLING OFFICE NAME AND ADDRESS Dr. T.E. Luke AFIT-EN WPAFB, Dayton, Ohio 45433		12. REPORT DATE March 1983 13. NUMBER OF PAGES 63
14. MONITORING AGENCY NAME & ADDRESS(if different from Controlling Office)		15. SECURITY CLASS. (of this report) Unclassified 15a. DECLASSIFICATION/DOWNGRADING SCHEDULE

16. DISTRIBUTION STATEMENT (of this Report)

Approved for public release; distribution unlimited

17. DISTRIBUTION STATEMENT (of the abstract entered in Block 20, if different from Report)

18. SUPPLEMENTARY NOTES

Approved for public release IAW AFR 190-17.

LYNN E. WOLAVER
Dean for Research and Professional Development
Air Force Institute of Technology (ATC)
Wright-Patterson AFB OH 45433

7 APR 1983

19. KEY WORDS (Continue on reverse side if necessary and identify by block number)

Laser Induced Resonance Fluorescence
Thermionic Dispenser Catjode
Calcium Evaporation

20. ABSTRACT (Continue on reverse side if necessary and identify by block number)

Three methods, laser induced resonance fluorescence, excitation to a shorter lived level from a metastable level, ionization spectroscopy are examined for feasibility of detecting and measuring calcium evaporation from a type B cathode. Laser induced fluorescence of the $4s\,^1S_0 \rightarrow 4p\,^1P_1$ (4226 Å) transition of calcium is the most promising and the easiest to implement. Ionization of the calcium atoms after they have been excited by a laser to the metastable $^3P_1$ state is feasible but requires redesign

DD FORM 1 JAN 73 1473 EDITION OF 1 NOV 65 IS OBSOLETE

SECURITY CLASSIFICATION OF THIS PAGE (When Data Entered)

of extant equipment to implement. Excitation to a shorter lived level from the metastable $^3P_1$ state is feasible for the transition from the $^3D_2$ (4435Å) level and not feasible for the $^3S_1$ (6122Å) transition. Sensitized fluorescence and stimulated emission involving excited calcium atoms is examined and discarded. Calcium evaporation rates are semi-quantitatively related to barium evaporation rates to take advantage of the more extensive literature on the latter. Limited experimental data is presented which indicates that an observation reported by another researcher of the barium evaporation rate decreasing after the cathode exceeded 1200°K is not attributable to pulse pile up error in the photon counting system but is most likely attributable to a cathode physics phenomenon. An argument for switching the course of future experiments from evaporation rate vs lifetime studies to evaporation rate vs temperature is made. All calculations are based upon experimental of previous workers and are order of magnitude rather than a rigorous treatment.